

RESEARCH

Open Access



# Microwave assisted drug delivery of titanium dioxide/rose Bengal conjugated chitosan nanoparticles for micro-photodynamic skin cancer treatment in vitro and in vivo

Samir Ali Abd El-Kaream<sup>1</sup>, Nasser Ali Mohamed Hassan<sup>2</sup>, Hassan Saleh Abdullatif Saleh<sup>3</sup>, Mohamed Albahloul Salem Albahloul<sup>3</sup>, Abdalla Mohamed Khedr<sup>3</sup> and Sohier Mahmoud El-Kholey<sup>2\*</sup>

## Abstract

**Background** Micro-photodynamic therapy (MWPDT) combines photo-dynamic (PDT) and microwave-dynamic (MWDT) therapies with sensitizers, offers new avenues for cancer treatment. Despite the fact that novel sensitizers for MWPDT have been successfully synthesized, only a few are being employed effectively. The low tumor-targeting specificity, inability to transport sensitizer's deeper intratumorally, and deteriorating tumor microenvironment all restrict their anti-tumor efficacy. The current work was done aiming at microwave assisted drug delivery of titanium dioxide / rose Bengal conjugated chitosan nanoparticles (TiO<sub>2</sub>/RB@CSNP) for micro- photo-dynamic skin cancer (SKCA) treatment in vitro and in vivo as activated cancer treatment up-to-date modality.

**Materials and methods** The study was conducted in vitro on human SKCA cells (A-375) and the study protocol application groups in vivo on Swiss albino mice treated with 7,12-dimethylbenz[a]anthracene (DMBA)/croton oil only and were not received any treatment for inducing SKCA, and only after SKCA induction the study treatment protocol began, treatment was daily with TiO<sub>2</sub>/RB@CSNP as MWPDT sensitizer with or without exposure to laser (IRL) or microwave (MW) or a combination of them for 3 min for two weeks.

**Results** Revealed that CSNP can be employed as effective TiO<sub>2</sub>/RB delivery system that directly targets SKCA cells. Additionally TiO<sub>2</sub>/RB@CSNP is a promising MWPS for and when combined with MWPDT can be very effective in treatment of SKCA-A-375 in vitro (cell viability decreased in a dose-dependent basis, the cell cycle progression in G<sub>0</sub>/G<sub>1</sub> was slowed down, and cell death was induced as evidenced by an increase in the population of Pre-G cells, an increase in early and late apoptosis and necrosis, and an increase in autophagic cell death) and DMBA/croton oil SKCA-induce mice in vivo (induced antiproliferative genes (caspase 3,9, p53, Bax, TNFalpha), suppressed antiapoptotic and antiangiogenic genes (Bcl2,VEGF respectively) effectively reducing the tumors growth and leading to cancer cell death as well as decreased oxidative stress (MDA), and ameliorated enzymatic and non-enzymatic antioxidants (SOD, GR, GPx, GST, CAT, GSH, TAC) as well as renal (urea, creatinine) and hepatic (ALT, AST) functions. This process could be attributed to MWPDT; microwave and/or photo-chemical TiO<sub>2</sub>/RB activation mechanism and antioxidant potential of non activated TiO<sub>2</sub>/RB as well.

\*Correspondence:

Sohier Mahmoud El-Kholey  
Dandana.2015@yahoo.com

Full list of author information is available at the end of the article



© The Author(s) 2025. **Open Access** This article is licensed under a Creative Commons Attribution 4.0 International License, which permits use, sharing, adaptation, distribution and reproduction in any medium or format, as long as you give appropriate credit to the original author(s) and the source, provide a link to the Creative Commons licence, and indicate if changes were made. The images or other third party material in this article are included in the article's Creative Commons licence, unless indicated otherwise in a credit line to the material. If material is not included in the article's Creative Commons licence and your intended use is not permitted by statutory regulation or exceeds the permitted use, you will need to obtain permission directly from the copyright holder. To view a copy of this licence, visit <http://creativecommons.org/licenses/by/4.0/>.

**Conclusion** The results indicate that TiO<sub>2</sub>/RB@CSNP has great promise as an innovative, effective delivery system for selective localized treatment of skin cancer that is activated by MWPDT.

**Keywords** Skin cancer, Chitosan nanoparticle, Titanium dioxide, Rose Bengal, Micro-photodynamic

## Introduction

One of the most commonly diagnosed cancers groups worldwide is skin cancers (SKCAs) [1]. Global statistics from the SKCA Foundation indicate that one out of every three cancer diagnoses is a SKCA. Epidermis is made from keratinocytes, the predominant skin cells with melanocytes spread into the basal layer between the keratinocytes. The other cell types are rare and more present in the subepidermal layers and in the follicular structures. Also hypodermis is situated beneath the dermis and is a part of the skin. Any abnormality in this specific area of the skin could lead to a number of negative outcomes, such as the emergence of SKCA. SKCA is classified into two main categories: non-melanoma (NM) SkCA and melanoma (M) SKCA [1, 2]. Globally, NMSKCA is the most commonly diagnosed cancer kind, and MSKCA is associated with the highest number of deaths from cancer. In Egypt, 5% of all malignant tumors in the body were SKCAs. In Egypt, squamous cell carcinomas (SCC) account for 15% of cases, while melanomas account for 8% of cases. Basal cell carcinomas, or BCCs, account for 77% of all cases [1–4].

Nowadays, among other methods, SKCA is treated using radiation therapy, chemotherapy, cryosurgery, or surgical excision. There are benefits and drawbacks to each of the many treatment modalities, so selecting a course of action is never simple and is determined by a number of circumstances. Diligent research and the development of novel treatments for malignant tumors can improve the overall survival rate of SKCA patients. The use of therapeutic nano-formulation offers an alternate tactic to mitigate the harmful effects of synthetic materials [5, 6]. Furthermore, cutting-edge methods for treating malignant tumors are being actively studied and developed, which enhances patient survival in general. Micro-photo-dynamic therapy (MWPDT) is an alternate therapeutic approach for SKCA that use sensitizer in conjunction with microwave and photo-irradiation of the tumor to treat the condition. In order to initiate a variety of biological processes in the diseased area, MWPDT entails first giving a MWPS and then exposing the area to light and microwaves with the same absorbance wavelength as the MWPS to produce highly reactive oxygen species (ROS), such as peroxides (R–O–O<sup>•</sup>), hydroxyl radicals (<sup>•</sup>OH), and singlet oxygen (<sup>1</sup>O<sub>2</sub>), which cause irreversible damage to cancer cells. MWPDT inspired by photodynamic therapy (PDT), Micro-dynamic treatment

(MWDt) has drawn interest as a potentially beneficial noninvasive treatment. PDT is ineffective in treating deeply embedded cancers due to its poor depth of light penetration. However, MWDt's main benefit over PDT is its ability to target soft tissue precisely and penetrate it up to tens of centimeters deep. MWDt thus resolves the main issue with PDT. In recent years, the use of MWPDT to treat a variety of tumors has grown in popularity, either by itself or in combination with other forms of treatment [7–11].

Titanium dioxide (TiO<sub>2</sub>) is one of the most basic materials in daily life that represents tremendous photo-catalyst activity. Recently, several functionalized biodegradable polymers were recently designed for TiO<sub>2</sub> nanoparticles-based photo-thermal and photodynamic therapies. These photosensitizers can be modified by attaching dyes, targeting molecules, and drug molecules. Rose Bengal (4,5,6,7-tetrachloro-20,40,50,70-tetraiodo-fluorescein disodium, RB) is a dye belonging to the fluorescein family. This amphiphilic chemical molecule is already used in medical applications to test the activity of the liver and to diagnose corneal lesions. Subsequently, it had been discovered by researchers that RB stimulates the immune system, and making it possible to reduce the risk of certain cancers [12, 13].

Many sensitizers, including Rose Bengal (RB), and titanium dioxide (TiO<sub>2</sub>), have been found to respond to light irradiation in addition to being microwave activated, which may have implications for anticancer therapy through producing deadly singlet oxygen after being exposed to irradiation, which kills tumor cells. The microwave can also increase the amount of mechanical stress that causes cellular membrane breakage, which can further boost the microwave's potential to kill cells. However, RB showed a quick rate of clearance and minimal tumor buildup, which significantly constrained the use of RB in in vivo settings going forward. To overcome its shortcomings, sensitizers can be precisely delivered to the targeted tumor site using nanoparticle-based drug delivery systems because of their improved retention and penetration; appropriately sized nanoparticles should passively target and accumulate in tumors. Among these systems, a natural polysaccharide called chitosan, a derivative of chitin, has gained considerable attention as a biocompatible, biodegradable, and mucoadhesive material for creating nanoparticles. Chitosan nanoparticles provide several advantages, including improved stability,

cellular uptake, solubility of anticancer drugs, modulation of release kinetics, and biodistribution. Additionally, chitosan nanoparticles can be modified on their surface with ligands or stimuli-responsive moieties to achieve targeted delivery to specific cancer cells or tissues. Furthermore, using MWPS's therapeutic substances in nanoformulations provides a substitute for the negative effects of synthetic medications [12–15].

Using biodegradable locally activated nanoparticles is another way to lessen the negative effects of traditional drugs. Additionally, state-of-the-art techniques for managing malignant tumors are continually being researched and developed, which improves overall patient survival. The anticancer properties of titanium dioxide/rose bengal chitosan based nanoparticles ( $\text{TiO}_2/\text{RB@CSNP}$ ) and their possible applications as MWPS for MWPDPT have not been well explored. Therefore, the main objective of the present work is to deliver a novel investigation to evaluate the microwave assisted drug delivery of titanium dioxide/rose bengal chitosan based nanoparticles for micro-photo-dynamic skin cancer treatment both in vitro and in vivo.

## Materials and methods

### Materials

Every chemical utilized came from a commercial source and didn't require any additional purification. Titanium tetra isopropoxide (TTIP), Chitosan, tripolyphosphate (TPP), Acetic acid, N-ethyl-N'-(3-dimethyl aminopropyl) carbodiimide (EDC), sodium hydroxide (NaOH), and N-hydroxysuccinimide (NHS) were obtained from (Sigma-Aldrich). Rose Bengal were acquired from Shanghai, China's Aladdin Industries Inc. Kits of antioxidant total capacity (TAC), glutathione-S-transferase, peroxidase and reductase (GST, GPx, GSR), Superoxide dismutase (SOD), catalase (CAT), aspartate, alanine aminotransferase (AST, ALT), urea and creatinine, were acquired from Biodiagnostic Cairo, Egypt, along with lipid peroxide (Malondialdehyde; MDA). The ABT (spin column) total RNA Mini extraction kit, ABT cDNA synthesis H-minus kit, and WizPure™ qPCR (SYBR) Master were acquired from Wizbiosolutions Inc. and Applied Biotechnology, respectively.

**Preparation and characterization of  $\text{TiO}_2/\text{RB@CSNP}$ :**  $\text{TiO}_2/\text{RB-CSNP}$  was utilized as MWPS in the current work Fig. (1).  **$\text{TiO}_2$  NP synthesis;** initially, 20 ml of ethanol solution are stirred continuously for 30 min to dissolve 0.1 N of TTIP. The dispersion medium was then created by adding a few drops of distilled water. The product spent twenty minutes in the ultrasonic bath. The solution was sonicated and then in an autoclave set at 150 °C placed for three hours. After the solution has reached room temperature, the contaminants were eliminated

by centrifuging and washing it with deionized water. Filter paper is then used to filter it. The filtered sample was annealed for two hours at 500 °C after being dried for five hours at 110 °C. The resulting  $\text{TiO}_2$  nanoparticles were gathered and subjected to further analysis. **Chitosan NP synthesis;** 50 ml of 5% acetic acid solution was added with one gram of chitosan flakes. To guarantee the chitosan flakes full dissolution, the chitosan viscous solution was vigorously stirred for 24 h using a magnetic stirrer. The resulting viscous solution was poured into a 1000 mL (0.5 M) NaOH solution in drops at a rate of 1 mL/min using a 10 mL syringe. To get rid of any remaining traces of NaOH solution, distilled water was used to wash the fresh chitosan beads.  **$\text{TiO}_2/\text{RB@CSNP}$  synthesis;** In order to initiate the crosslinking reaction, 90 mL of 1% TPP solution was added drop wise to the fresh chitosan beads while being heated in a water bath at 40 °C for two hours with moderate stirring. When crosslinking chitosan with TPP, the pH was adjusted to about 4. The cross-linked chitosan-tripolyphosphate beads (CSTPP) were then thoroughly cleaned with distilled water and allowed to air dry for a full day. Subsequently, the CSTPP beads were continually dried in the oven after being mashed with a mortar and pestle. The remaining CSTPP powder was intended for additional uses. Cross-linked chitosan-tripolyphosphate/ $\text{TiO}_2$  ( $\text{TiO}_2\text{-CSTPP}$ ) was created by loading  $\text{TiO}_2$  NP with chitosan flakes and then dissolving them in a 5% acetic acid solution in order to satisfy the optimization process's requirements. Conversely, RB was loaded onto chitosan after being chemically cross-linked to CSTPP using (5 mM) NHS and EDC. After dialyzing the  $\text{TiO}_2/\text{RB@CSNP}$  for one week (using cellulose tubing from Sigma and cutting off 12,000–14000 g/mol), the filtrate was freeze-dried [16–18].  $\text{TiO}_2/\text{RB-CSNP}$  was characterized by scanning photoluminescence and absorbance spectrometry (PL, UV/Visible), Fourier transform infrared scanning spectroscopy (FTIR), scanning energy dispersive and diffraction X-ray (EDX,XRD), transmission and scanning electron microscopy (TEM, SEM), particle size analyzer and zeta potential to measure its size and shape.  $\text{TiO}_2/\text{RB@CSNP}$  treated SKCA-A-375 cell lines and the DMBA/croton oil-SKCA-induced mice groups (painted topically) allowed to incubate for nine to twelve hours prior to being exposed to PDT and/or MWDT for two weeks.

### Methods

All applicable regulations and standards were adhered to during the entire investigation whole inquiry process.

### Ethics statement

Experimental procedures, animal handling and sampling followed the Guide for the Care and Use of Laboratory

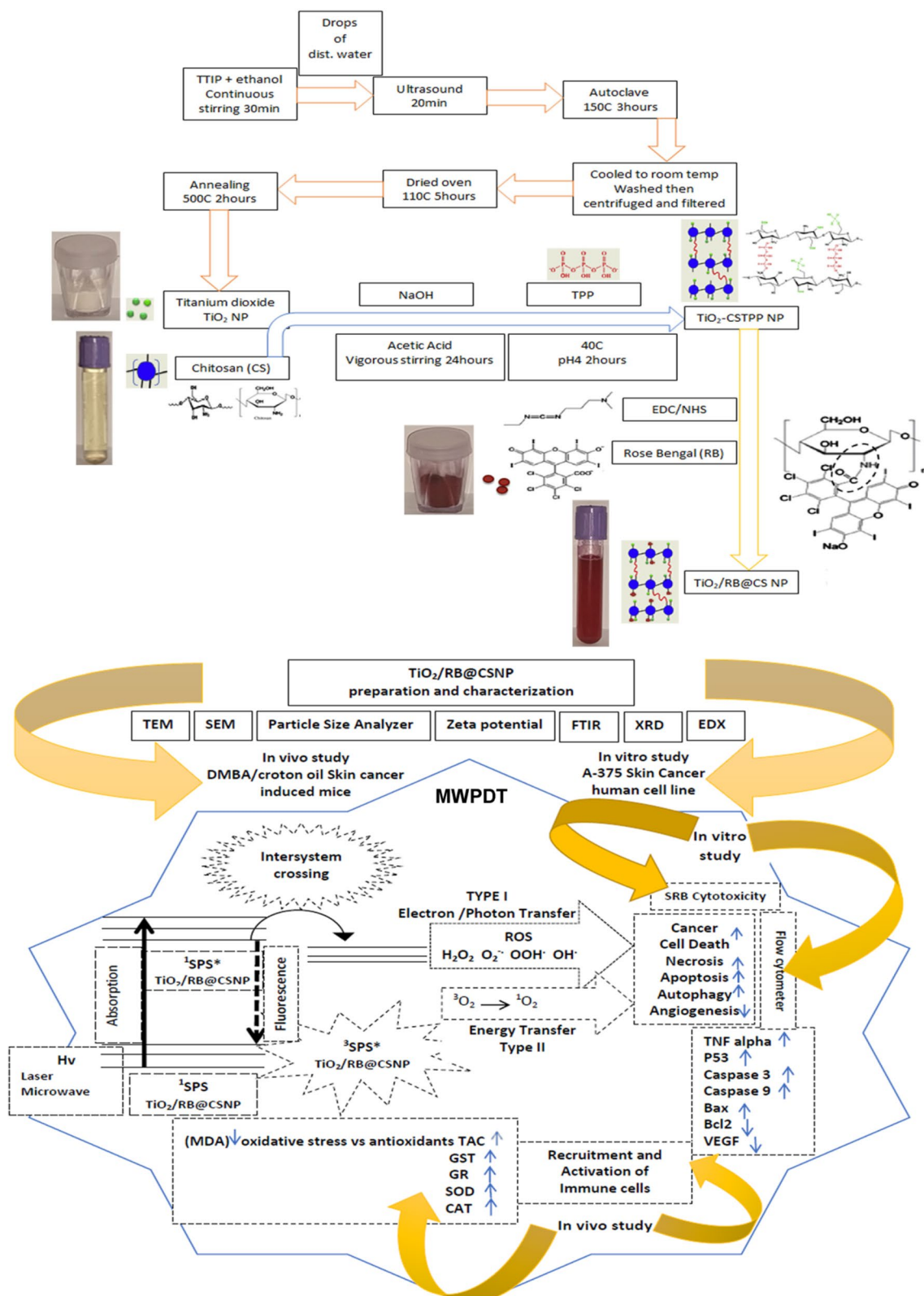


**Fig. 1** Schematic representation of TiO<sub>2</sub>/RB-CSNP synthesis and MWPDT

Animals and were approved by Research Ethical Committee [Institutional Animal Care and Use Committee, (ALEXU-IACUC; Code No.01219112821)] of the Medical Research Institute, Alexandria University (Alexandria, Egypt).

**In vitro study:** 1. (+ ve Control): SKCA cell line (A-375) was maintained in drug-free environment and were kept without treatment. 2. (TiO<sub>2</sub>/RB@CSNP without activation group): SKCA cell line (A-375) was treated with 0.033 µl TiO<sub>2</sub>/RB@CSNP only. 3. (Laser group): SKCA cell line (A-375) was exposed to laser, for 3 min. 4. (TiO<sub>2</sub>/RB@CSNP laser activated group): SKCA cell line (A-375) was treated with 0.033 µl TiO<sub>2</sub>/RB@CSNP and exposed to laser as group 3. 5. (Microwave group): SKCA cell line (A-375) was exposed to microwave for 3 min. 6. (TiO<sub>2</sub>/RB@CSNP microwave activated group): SKCA cell line (A-375) was treated with 0.033 µl TiO<sub>2</sub>/RB@CSNP and exposed to microwave as group 5. 7. (Laser and microwave combined group): SKCA cell line (A-375) was exposed laser and microwave for 3 min. 8. (TiO<sub>2</sub>/RB@CSNP laser and microwave combined activated group): SKCA cell line (A-375) was treated with 0.033 µl TiO<sub>2</sub>/RB@CSNP, exposed to laser and microwave as group 7.

**In vivo study:** Ninety Albino mice, with a weight range of 20 ± 5 g and of 60 ± 5 days, were acquired from the Faculty of Agriculture's animal house at Alexandria University. Mice were housed in appropriate cages with twelve wake-light/sleep-dark cycles and an ambient temperature of 25 ± 0.5 °C. The mice had unrestricted access to tap water and were fed a regular, consistent pellet diet. The medication was started after a week of acclimation for the mice. To put it briefly, nine groups of ten mice each were assembled from the mice: 1. (Negative Control group): Untreated normal, healthy mice were maintained. 2. (Positive SKCA Control group): mice were received topical painting of [(25 µg DMBA/0.1 ml acetone/mouse) twice weekly, then one week after the initiation with DMBA, (1% croton oil/0.1 ml acetone/mouse) was applied twice weekly] for eight weeks only to induce SKCA and maintained without treatment. 3. (TiO<sub>2</sub>/RB@CSNP without activation group): SKCA induced mice were treated by a daily dose of 0.033 ml of dissolved TiO<sub>2</sub>/RB@CSNP only. 4. (Laser exposed group): For two weeks, SKCA-induced mice were subjected to laser for three minutes every day. 5. (Laser activated TiO<sub>2</sub>/RB@CSNP group): SKCA induced mice were treated by a daily dose of 0.033 ml of TiO<sub>2</sub>/RB@CSNP per mouse and subsequently subjected to a laser for three minutes every day. 6. (Microwave exposed group): For two weeks, SKCA-induced mice were subjected to microwave for three minutes each day. 7. (Microwave activated TiO<sub>2</sub>/RB@CSNP group): SKCA-induced mice were treated by a daily dose of 0.033 ml of TiO<sub>2</sub>/RB@CSNP per mouse

and subsequently subjected to microwave for three minutes every day. 8. (Laser and microwave combination activated group): For two weeks, SKCA-induced mice were subjected to laser light, followed by microwave for three minutes every day. 9. (Laser and microwave combined activated TiO<sub>2</sub>/RB@CSNP group): SKCA-induced mice were treated by a daily dose of 0.033 ml TiO<sub>2</sub>/RB@CSNP per mouse, and were exposed to both laser and microwave for three minutes each day.

## Instruments

### Laser irradiation

A-375 cell line of each group was subjected to a three-minute laser therapy under the predetermined conditions in in vitro study section. For in vivo study; the mice were made anesthetic with 100, 10 mg/kg bw Ketamine and Xylazine respectively injection before to the laser exposure. The hair was shaved around the tumor. The mouse was placed with its back to the board. The probe was positioned almost atop the tumor exactly, and each group received a three-minute laser therapy under the predetermined conditions. After PDT, to prevent skin irritation mice were maintained in the dark. A laser LAS 250- Hi-Tech infrared diode type, fysiomed, China, with a peak 50 W output and a 600–904 nm wavelength of 7000 Hz frequencies, was utilized to expose the tumor in mice (10 mW and 0.43 J/cm<sup>2</sup>).

### Microwave irradiation

A-375 cell line of each group was subjected to a three-minute microwave therapy under the predetermined conditions in in vitro study section. For in vivo study; the mice were put to sleep with 100, 10 mg/kg bw Ketamine and Xylazine respectively injection before to being exposed to microwave irradiation. The hair around the tumor was shaved. The mouse tumor was placed with its back to the board. The probe was positioned almost exactly atop the tumor, and each group was subjected to a three-minute microwave therapy under the predetermined conditions. Mice tumors were exposed using a microwave (Microwave Diathermy Model HME-009, China) operated at +10 ~ + 70 ambient temperature, 30%–75%, relative humidity, 700 hPa ~ 1060 hPa atmospheric pressure, 220 ± 22 V 50 ± 1HZ power supply, 50 ± 1 Hz power frequency, rated output power: ≤ 100 W, output power ≤ 450 VA, 50 Ω matched load impedance).

When the study protocols was over, the mice were euthanized by inhaling 5% (overdose) isoflurane and immediately after 60 s as the animals no longer have a heartbeat and have whitish eyes, cervical dislocation was performed to ensure euthanasia. After the dissection, blood samples were taken in order to get whole blood and sera. One portion of the blood was centrifuged for

ten minutes at 1000xg, and the separated sera were kept until analysis at  $-20^{\circ}\text{C}$ . The leftover blood sample was collected and maintained until the analysis of genes relative expressions identification was initiated at  $-80^{\circ}\text{C}$ . It was then transferred from the vial containing EDTA to another vial containing RNA later solution. Additionally, SKCA tissues were taken out right away, cleaned in cold saline, pierced in a vial with a needle, and kept for histological analysis in 10% formalin/saline.

#### **Cell culture**

Human skin cancer A-375 cell line was provided from the American Type Culture Collection (ATCC). The cells were cultured at  $37^{\circ}\text{C}$  in a humidified 5% (v/v)  $\text{CO}_2$  environment in DMEM medium supplemented with 10% heat-inactivated fetal bovine serum, 100 units/mL of penicillin and 100 mg/mL streptomycin.

#### **Assay for cytotoxicity and cell viability**

The cytotoxic effect of  $\text{TiO}_2/\text{RB}@/\text{CSNP}$  against A-375 cells was assessed using the sulforhodamine B (SRB) test. After 100  $\mu\text{L}$  ( $5 \times 10^3$  cells) aliquots of cell suspension were planted on 96-well plates, the entire medium was incubated for 24 h. The cells were treated with a further aliquot of 100  $\mu\text{L}$  media with  $\text{TiO}_2/\text{RB}@/\text{CSNP}$  at various doses (1000, 100, 10, 1.0, and 0.1  $\mu\text{M}$ ). After being exposed to various modalities for 24 h, with and without  $\text{TiO}_2/\text{RB}@/\text{CSNP}$ , the cells were fixed by replacing the media with 150  $\mu\text{L}$  of 10% TCA and incubated for one hour at  $4^{\circ}\text{C}$ . Following the removal of the TCA solution, the cells were washed five times with distilled water. Aliquots of 70  $\mu\text{L}$  (0.4% w/v) SRB solution were added, and they were then left to sit at room temperature in a dark place for ten minutes. The plates were allowed to air dry for the full night following three washing with 1% acetic acid. The protein-bound SRB stain was then dissolved with 150  $\mu\text{L}$  (10 mM) of TRIS, and the absorbance at 540 nm was measured using a LABTECH.<sup>®</sup>-FLUOstar BMG Omega microplate reader (Ortenberg, Germany) [19].

#### **Flow cytometer assay**

##### **Cell cycle analysis**

After being treated with different modalities for 24 h, both with and without  $\text{TiO}_2/\text{RB}@/\text{CSNP}$ , A-375 cells ( $10^5$  cells) were collected by trypsinization. After that, the cells were twice cleaned in ice-cold PBS (pH 7.4). The cells were fixed for an hour at  $4^{\circ}\text{C}$  after being re-suspended in two milliliters of 60% ice-cold ethanol. The fixed cells were first suspended in 1 mL of PBS with 10  $\mu\text{g}/\text{mL}$  propidium iodide (PI) and 50  $\mu\text{g}/\text{mL}$  RNAase A, and then they were repeatedly washed in PBS (pH 7.4). After incubating in the dark for 20 min at  $37^{\circ}\text{C}$ , the cells were analyzed by flow cytometer using an ACEA Novocyt<sup>™</sup> flow

cytometer (ACEA Biosciences Inc., San Diego, CA, USA) equipped with a FL2 ( $\lambda_{\text{ex/em}}$  535/617 nm) signal detector to ascertain the DNA content of the cells. For every sample, a total of 12,000 events were collected. The cell cycle distribution was ascertained using ACEA NovoExpress.<sup>™</sup> software (San Diego, ACEA Biosciences Inc., CA, USA) [20].

##### **Analysis of necrosis and apoptosis in Annexin V-FITC/PI**

The populations of necrosis and apoptosis cells were identified using two fluorescent channels flow cytometer in combination with the Abcam Inc., Cambridge Science Park, Cambridge, UK, Annexin V-FITC apoptosis detection kit. Following a 24-h period of treatment with various modalities both with and without  $\text{TiO}_2/\text{RB}@/\text{CSNP}$ , A-375 cells ( $10^5$  total) were isolated using trypsinization and twice washed in pH 7.4 ice-cold PBS. Cells were treated with 0.5 ml of Annexin V-FITC/PI solution for 30 min at room temperature in the dark, as per the manufacturer's instructions. Following staining, the fluorescence signals for FITC and PI were evaluated using FL1 and FL2 signal detectors ( $\lambda_{\text{ex/em}}$  488/530 nm for FITC and  $\lambda_{\text{ex/em}}$  535/617 nm for PI), respectively, using Novocyt<sup>™</sup> ACEA flow cytometer. For each sample, a total of 12,000 events were recorded. Positive FITC and/or PI cells were computed and quantified using quadrant analysis using NovoExpress.<sup>™</sup> ACEA software [21].

##### **Autophagy analysis**

Acridine orange (AO), a lysosomal dye, and flow cytometer analysis were used to quantify autophagic cell death. Trypsinization was used to extract A-375 cells ( $10^5$  cells) after different modalities were used for 24 h, both with and without  $\text{TiO}_2/\text{RB}@/\text{CSNP}$ . After that, the cells were twice cleaned in ice-cold PBS (pH 7.4). The cells were stained with acridine orange (10  $\mu\text{M}$ ) and then incubated at  $37^{\circ}\text{C}$  in the dark for 30 min. After labeling, cells were injected using a Novocyt<sup>™</sup> ACEA flow cytometer, and the acridine orange fluorescent signals were analyzed using the FL1 signal detector ( $\lambda_{\text{ex/em}}$  488/530 nm). For each sample, 12,000 events were gathered, and net fluorescence intensities (NFI) are measured using NovoExpress.<sup>™</sup> ACEA software [22].

##### **Migration (Wound healing) assay**

Using a cell scratch assay, the effect of  $\text{TiO}_2/\text{RB}@/\text{CSNP}$  on A-375 cell migration was examined. A-375 cells were seeded onto a coated 12-well plate at a density of  $2 \times 10^5$ /well for the scratch wound assay. After that, they were grown in 5% FBS-DMEM for the whole night at  $37^{\circ}\text{C}$  and 5%  $\text{CO}_2$ . The next day, horizontal scratches were applied to the confluent monolayer. After that, PBS was used to thoroughly clean the plate. New media containing

activated TiO<sub>2</sub>/RB@CSNP was added to the treatment wells, and fresh medium was added to the control wells. At predetermined intervals, pictures were taken with an inverted microscope. The plate was incubated at 37 °C with 5% CO<sub>2</sub> in between time intervals. Version 3.7 of the MII ImageView program displays and analyses the obtained images [23].

### Histological, molecular, and biochemical analyses

#### *Examination of the Liver and Kidney Enzymes Biochemically*

Using commercial kits, kidney (creatinine, and urea) and the liver (AST, and ALT) enzymes were tested in accordance with Burtis et al. [24].

#### *Determination of the antioxidant markers and oxidative stress (oxidants)*

The levels of antioxidant markers and oxidants in the serum were assessed using commercial kits. Malondialdehyde (MDA), which are implied to predicting lipid peroxidation [25]. SOD activity [26] glutathione- peroxidase, S-transferase, and reductase (GPx, GST, GR) activities [27, 28], Catalase activity [29, 30], Total antioxidant activity (TAC) [31].

#### *Evaluation of Caspase (3, 9), p53, Bax, Bcl-2, TNF alpha, and VEGF relative gene expressions*

QRT-PCR was used to determine genes expressions. Total RNA from blood samples was isolated using the ABT Total RNA Mini spin column extraction kit according to the directions. Purity by measuring the absorption 260/280 nm ratio was determined, which was usually greater than 1.8. As directed by the cDNA synthesis ABT H-minus kit, the cDNA was produced using an RT-PCR one-step reaction. For qRT-PCR, qPCR Master Wiz-Pure™ (SYBR) with ROX Dye was utilized. A reaction (20 μL) mixture using the template (5 μL) C-DNA and target gene primers (0.25 μM) P53-R: TGGAATCAACCCACA GCTGCA, CTGTCATCTTCTGTCCCTTC is P53-F, Caspase3-R: AAATGACCCCTTCATCACCA, TGTCAT CTCGCTCTGGTACG is Caspase3-F, Caspase9-F: AGT TCCCGGGTGCTGTCTAT, GCCATGGTCTTTCTG CTCAC is Caspase9-R, TNF-α-R: TGAGATCCATGC CGTTGGC, CACGTCGTAGCAAACCACC is TNF-α-F: Bax-R: CCAGTTCATCTCCAATTCG, CTACAG GGTTCATCCAG is Bax-F, Bcl2-F: GTGGATGACTGA GTACCT. CCAGGAGAAATCAAACAGAG is Bcl2-R, VEGF-R: TTTCTCCGCTCTGAACAAGG, AAAAAC GAAAGCGCAAGAAA is VEGF-F, using qRT-PCR Sybr Green (10 μL) and β-actin-R (CTCTCAGCTGTG GTGGTGAA) and β-actin-F (AGCCATGTACGTAGC CATCC) was utilized. 35 cycles were employed in each run of PikoReal Thermo Scientific's qRT-PCR apparatus (PR0241401024), with 10 s at 95 °C, 10 s at 55 °C, and 5 s

at 72 °C. The initial denaturation was done for five minutes at 95 °C. The identical sample β-actin mRNA levels were used to compare all of the gene expressions, and the fold difference was calculated using the Eq.  $2^{-\Delta\Delta C_t}$  previously mentioned [32].

#### *SKCA tissue histopathology analyses*

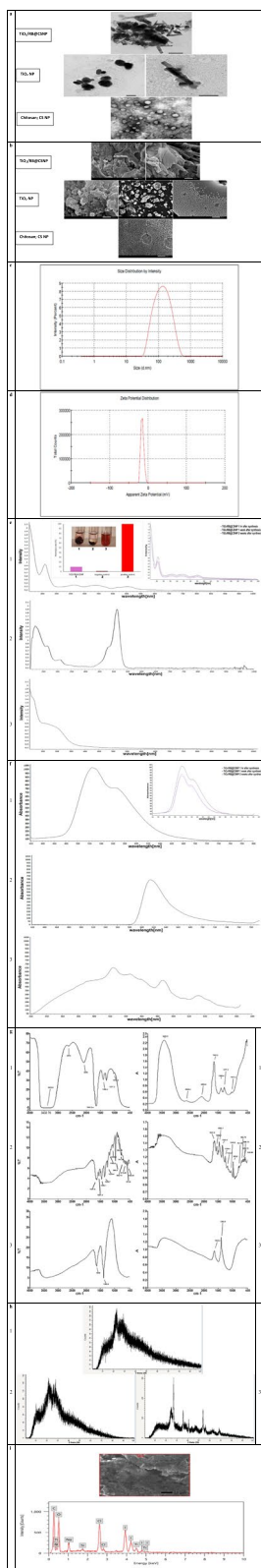
After being embedded in paraffin, the gathered SKCA samples were sectioned into sections after being fixed by soaking them in a formalin/saline (10%) solution. To ascertain the extent of the histological changes in the SK tissue, eosin and hematoxylin (H&E) staining dye was used. Every slide was inspected and photographed using a light microscope [33].

**For statistical analysis**, the data was given as mean ± standard deviation (SD). One-way analysis of variance (ANOVA) was used to confirm the statistical variances of the data. To establish statistical significance, a *p* value of less than 0.05 was utilized. To compare groups, SPSS 25.0's post hoc analysis function was utilized.

## Results

### *Characterization of TiO<sub>2</sub>/RB@CSNP*

In accordance with the particle size of TiO<sub>2</sub>/RB@CSNP demonstrated by TEM as well as particle size analyzer Fig. (2a,c), SEM results showing porous surface morphology of TiO<sub>2</sub>, CSNP and illustrating the conjugation of TiO<sub>2</sub>/RB to CSNP Fig. (2b), zeta potential results Fig. (2d), optimum characteristic (UV-Visible) absorption peaks for TiO<sub>2</sub> and RB before and after conjugation with CSNP Fig. (2e), optimum characteristic (PL) photoluminescence peaks for TiO<sub>2</sub> and RB before and after conjugation with CSNP Fig. (2f), characteristic FTIR bands found that match the vibrations of the functional groups that are present in TiO<sub>2</sub> and RB before and after conjugation with CSNP represented on Fig. (2g); the FTIR spectra of TiO<sub>2</sub> in the range of 450–4000 cm<sup>-1</sup>, the peaks at 3432.8 and 1638 cm<sup>-1</sup> in the spectra are due to the stretching and bending vibration of the -OH group. In the spectrum of pure TiO<sub>2</sub>, the peaks at 523.88 cm<sup>-1</sup> show stretching vibration of Ti–O and peaks at 1382 cm<sup>-1</sup> shows stretching vibrations of Ti–O–Ti. RB-FTIR peaks at (1631.8, 1556.1, 1452.1, 1343.4, 1239.4, 1163.8, 1045.5, 955.8, 761.98, 670.72, 662.72, 568.18, 535.09) peak near 1614 cm<sup>-1</sup> could be attributed to carbonyl stretching (C–O) vibrations and the other three strong peaks in the ranges of 1300–1600 cm<sup>-1</sup> correspond to the (C–C) stretching vibrations. The pure CS FTIR spectrum several characteristic peaks at 3360, 2919, 2874, 1641.2, 1592, 1395.6, 127.2, 1153, 1017.2 and 893 cm<sup>-1</sup>, around 901 and 1155 cm<sup>-1</sup>, assigned to the saccharine structure and an amino and amid characteristic peak at 1592 cm<sup>-1</sup>. There was a stronger absorption band at 1641 corresponding to



◀ **Fig. 2** Characterization of TiO<sub>2</sub>/RB@CSNP; **a**, TEM, **b**, SEM, **c**, particle size, **d**, zeta potential of TiO<sub>2</sub>/RB@CSNP, **e**, UV-Vis spectra, **f**, PL, **g**, FTIR transmittance and absorbance, **h**, XRD of (1. TiO<sub>2</sub>/RB@CSNP, 2. RB, 3. TiO<sub>2</sub>), **i**, EDX of TiO<sub>2</sub>/RB@CSNP

the carbonyl of CS, as well as characteristic XRD peaks observed at 2θ value of TiO<sub>2</sub> 2θ at peak (25.46°, 27°, 36.32°, 40.79°, 44.89°, 54.91°, 55.75°, 67.63°, 68.38°) and RB 2θ at peak (7.82°, 8.48°, 12.25°, 14.68°, 16.25°, 18.267°, 20.61°, 22.59°, 26.85°) before and after conjugation with CSNP exhibit very broad peaks at 2θ = 10° and 2θ = 20° indicating crystallinity and phase purity of prepared TiO<sub>2</sub>/RB@CSNP CSNP Fig. (2 h), and EDX elemental analysis illustrating the presence of C in the CSNP in correct state alongside with Ti, O, N TiO<sub>2</sub>/RB content Fig. (2i), demonstrating the correct and well preparation of TiO<sub>2</sub>/RB@CSNP as well as correct conjugation and nanocomposite formation in nanoscale. The overall results indicated that consistent with earlier research, TiO<sub>2</sub>/RB@CSNP was synthesized successfully [16–18].

**Cytotoxicity of PDT, MWDT and MWPDT in presence and absence of (TiO<sub>2</sub>/RB@CSNP) upon treatment of SKCA A-375 cell line**

The cytotoxic effect of different activation modalities with and without TiO<sub>2</sub>/RB@CSNP was investigated in SKCA A-375 cells after 24 h treatments using the SRB viability assay. The SKCA A-375 cell line underwent treatment with varying TiO<sub>2</sub>/RB@CSNP doses and different activation modalities, which led to a rise in the number of floating cells and a change in cellular morphology. Additionally, the SRB test was used to evaluate PDT, MWDT, and MWPDT in the presence and absence of TiO<sub>2</sub>/RB@CSNP cytotoxicity, our findings revealed that the TiO<sub>2</sub>/RB@CSNP decrease proliferation of SKCA A-375 cell in a dose-dependent manner. In addition, the cytotoxicity analysis results of the current study manifested that the SKCA A-375 cell line was slightly affected by treatment with TiO<sub>2</sub>/RB@CSNP without activation followed by the SKCA A-375 cell line treated with lasers, microwave without TiO<sub>2</sub>/RB@CSNP. The SKCA A-375 cells cytotoxic effectiveness and growth inhibition owing to laser (PDT) and the microwave (MWDT) are both improved by the presence of TiO<sub>2</sub>/RB@CSNP. The acquired results demonstrated that both with and without the TiO<sub>2</sub>/RB@CSNP, MW is more cytotoxic effective than IRL against SKCA A-375 cell line. For integration with IRL, MW was chosen. In comparison to employing IRL or MW alone, the combination therapy approach (MWPDT) in presence of TiO<sub>2</sub>/RB@CSNP is most cytotoxic effective against SKCA A-375 cell line. Plotting cell viability vs. concentration yielded the concentration at

which the viable cells inhibited 50% by  $\text{TiO}_2/\text{RB}@CSNP$  (IC50), which was determined in  $\mu\text{g}/\text{ml}$  Fig. (3).

#### Cell cycle distribution effect of PDT, MWDT and MWPDT in presence and absence of ( $\text{TiO}_2/\text{RB}@CSNP$ ) upon treatment of SKCA A-375

When SKCA A-375 cells are treated with  $\text{TiO}_2/\text{RB}@CSNP$  at an IC50 equivalent concentration, a rise in the cell population at the G1 phase has been observed. The SKCA A-375 cell line was slightly affected by treatment with  $\text{TiO}_2/\text{RB}@CSNP$  without activation exhibited increase the cell population at the G1 phase and resulted in cell death manifested by Sub G1 phase increase and reciprocally, caused S phase and G2/M phase decrease followed by the SKCA A-375 cell line treated with lasers, microwave without  $\text{TiO}_2/\text{RB}@CSNP$ . The effectiveness SKCA A-375 cells distribution, arrest and growth inhibition owing to laser (PDT) and the microwave (MWDT) are both improved by the presence of  $\text{TiO}_2/\text{RB}@CSNP$  exhibited increase the cell population at the G1 phase and resulted in cell death manifested by Sub G1 phase increase and reciprocally, caused S phase and G2/M phase decrease. The acquired results demonstrated that both with and without the  $\text{TiO}_2/\text{RB}@CSNP$ , RF is more effective than IRL against SKCA A-375 cell line. For integration with IRL, MW was chosen. In comparison to employing IRL or MW alone, the combination therapy approach (MWPDT) in presence of  $\text{TiO}_2/\text{RB}@CSNP$  is most effective against SKCA A-375 cell line exhibited cell population increase at the G1 phase and resulted in cell death manifested by Sub G1 phase increase and reciprocally, caused S phase and G2/M phase decrease Fig. (4).

#### Apoptosis and necrosis cell death mechanism of PDT, MWDT and MWPDT in presence and absence of ( $\text{TiO}_2/\text{RB}@CSNP$ ) upon treatment of SKCA A-375

The SRB test and microscopic examination point to an apoptotic reaction to  $\text{TiO}_2/\text{RB}@CSNP$  as the possible cause of the decrease in cell viability. To gain additional knowledge about the mechanism underlying cell death (apoptosis versus necrosis), SKCA A-375 cells were treated with different activation modalities in presence and absence of  $\text{TiO}_2/\text{RB}@CSNP$  for 24 h. The treated cells' flow cytometer histogram revealed a population

shift that progressed from living cells in the lower left quadrant to early apoptosis in the lower right and finally from late apoptosis in the upper right quadrant to cell necrosis in the upper left. The treated cells also showed increase of annexin V positivity. SKCA A-375 cells treated with either  $\text{TiO}_2/\text{RB}@CSNP$  without activation or with lasers and microwave without  $\text{TiO}_2/\text{RB}@CSNP$  showed a substantial elevation in the percentage of cells exhibiting early and late apoptosis. In SKCA A-375 cells treated with laser (PDT) and microwave (MWDT), the addition of  $\text{TiO}_2/\text{RB}@CSNP$  increases both the elevation in the percentage of cells with early and late apoptosis. The obtained data showed that MW is more effective than IRL at raising the proportion of SKCA A-375 cells with early and late apoptosis, both with and without the  $\text{TiO}_2/\text{RB}@CSNP$ . For integration with IRL, MW was chosen. The combination MWPDT therapy approach in  $\text{TiO}_2/\text{RB}@CSNP$  presence is the most effective way to increase the proportion of SKCA A-375 cells with early and late apoptosis, as compared to using IRL or MW alone. Comparable observations were found for the percentage of necrotic cells in SKCA A-375 cells treated with either  $\text{TiO}_2/\text{RB}@CSNP$  without activation or with lasers and microwave without  $\text{TiO}_2/\text{RB}@CSNP$ . The inclusion of  $\text{TiO}_2/\text{RB}@CSNP$  improves both the elevation in the necrotic cells percentage of SKCA A-375 cells treated with microwave (MWDT) and laser (PDT). The obtained data showed that MW is more effective than IRL at increasing the proportion of necrotic SKCA A-375 cells, both with and without the  $\text{TiO}_2/\text{RB}@CSNP$ . The combined therapy strategy (MWPDT) in the presence of  $\text{TiO}_2/\text{RB}@CSNP$  is most successful in elevating the percentage of SKCA A-375 cells with necrosis as compared to using IRL or MW alone Fig. (5).

#### Autophagy cell death mechanism of PDT, MWDT and MWPDT in presence and absence of ( $\text{TiO}_2/\text{RB}@CSNP$ ) upon treatment of SKCA A-375

The SRB assay and microscopic examination indicate that program cell death other than apoptosis by autophagy in response to  $\text{TiO}_2/\text{RB}@CSNP$  may be the cause cell viability decline. For further exploration the process of cell death (autophagy), SKCA A-375 cells were subjected to different activation modalities for duration of 24 h, both

(See figure on next page.)

**Fig. 3** The effect of different treatment modalities on skin cancer (A-375) cell viability; Cells were exposed to different treatment modalities with serial dilution of  $\text{TiO}_2/\text{RB}@CSNP$  for 24 h, **a.** microscopic investigations, **b.** A375 containing  $\text{TiO}_2/\text{RB}@CSNP$  (arrow), Ne; nuclear envelop, Pm; plasma membrane, m; mitochondria, rer; rough endoplasmic reticulum and **c.** dose response curve in all in vitro study groups; cell viability was determined using SRB assay. cell viability (%):  $F = 5.822$   $p < 0.001^*$ . Mean  $\pm$  SD is used to illustrate the results ( $n = 3$ ). F stands for the ANOVA test value. <sup>a,b,c,d,e</sup> Significance to (skin cancer untreated group,  $\text{TiO}_2/\text{RB}@CSNP$  treated non activated group, laser-, microwave-, laser + microwave- exposed groups)

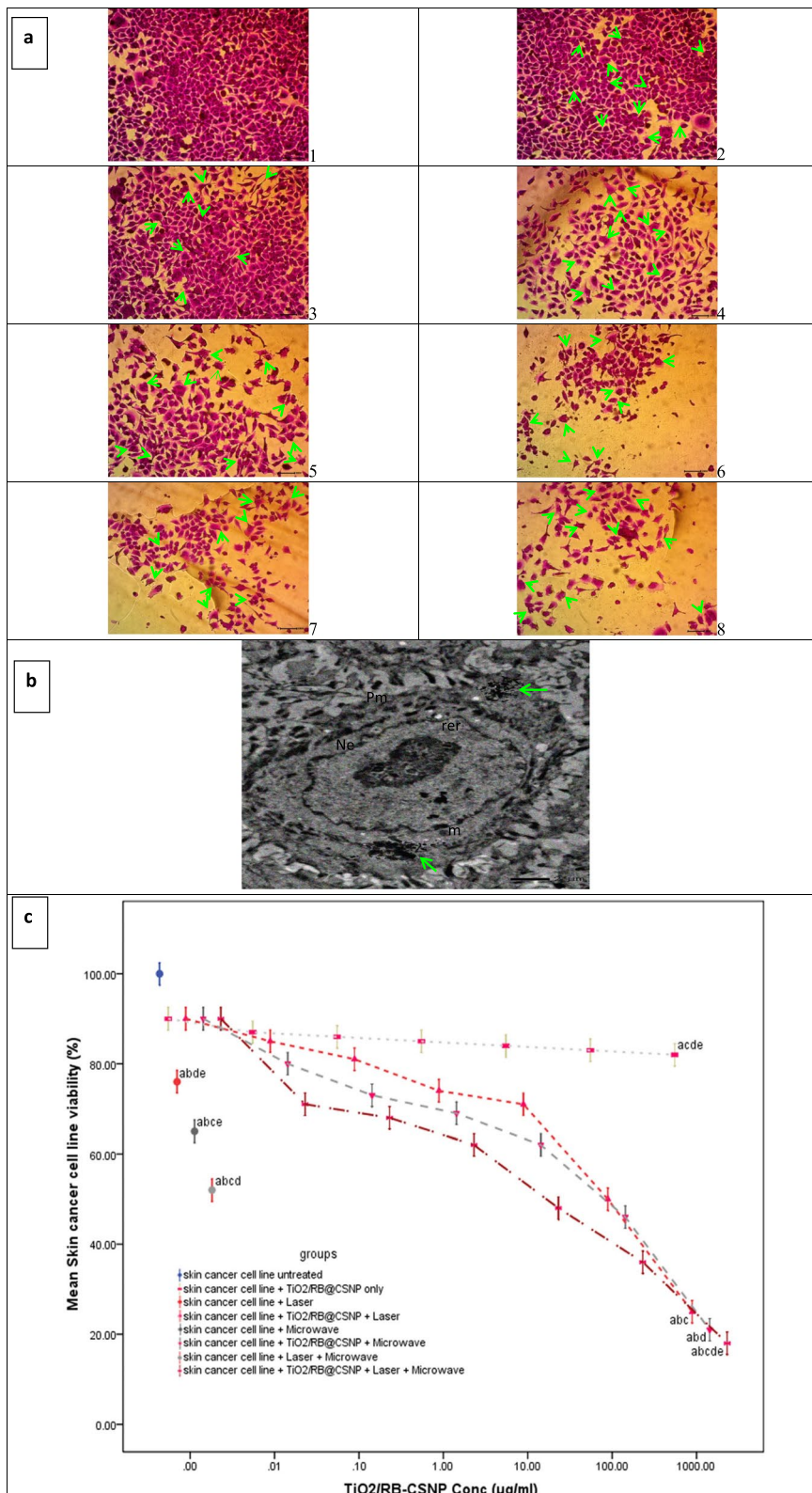


**Fig. 3** (See legend on previous page.)

in the presence and absence of TiO<sub>2</sub>/RB@CSNP. The treated cells expressed redder and less green when AO, a fluorophore that accumulates at high concentrations in acidic vesicular organelles (AVO) such as auto-lysosomes, dimerizes and causes a green to red metachromatic shift, that could be measured to study autophagy. SKCA A-375 cells treated with either TiO<sub>2</sub>/RB@CSNP without activation or with lasers and microwave without TiO<sub>2</sub>/RB@CSNP showed a substantial elevation in the percentage of cells undergoing autophagy. The presence of TiO<sub>2</sub>/RB@CSNP increases the percentage of autophagous cells in SKCA A-375 cells treated with both microwave dynamic therapy (MWDT) and laser photodynamic therapy (PDT). The obtained data showed that MW is more effective than IRL at raising the percentage of SKCA A-375 cells undergoing autophagy, both with and without the TiO<sub>2</sub>/RB@CSNP. For integration with IRL, MW was chosen. The combined therapy strategy (MWPDT) in the presence of TiO<sub>2</sub>/RB@CSNP is most successful in elevating the percentage of SKCA A-375 cells undergoing autophagy as compared to using IRL or MW alone Fig. (6).

#### Cell migration inhibition mechanism of PDT, MWDT and MWPDT in presence and absence of (TiO<sub>2</sub>/RB@CSNP) upon treatment of CRCA SW-620

After 24 h of treatment, SKCA A-375 cells were used to study the inhibitory effect of various activation methods with and without TiO<sub>2</sub>/RB@CSNP on cell migration. Daily wound closure assessments were conducted using the scratch assay until the control, untreated cells closed after 72 h. Compared to the untreated control group, the SKCA A-375 cell line treated with the combination therapy strategy (MWPDT) in the presence of TiO<sub>2</sub>/RB@CSNP shown a significant decrease in SKCA A-375 cell migration, illustrating a possible anti-migratory impact Fig. (7).

#### (TiO<sub>2</sub>/RB@CSNP) of PDT, MWDT, MWPDT and oxidative stress in vivo SKCA models

Figure (8) displays the effects of TiO<sub>2</sub>/RB@CSNP; PDT, MWDT, and MWPDT on lipid peroxidation oxidative stress MDA parameter in each of the experimental groups' mice. When comparing the untreated DMBA/croton oil-SKCA-induced control mouse group to the

non-irradiated group of mice treated with TiO<sub>2</sub>/RB@CSNP alone, the MDA showed very modest alterations in the sera. The untreated DMBA/croton oil-SKCA-induced control animals had significantly greater values of this parameter compared to the control normal healthy mice. Furthermore, all DMBA/croton oil-SKCA-induced mice treated with laser, microwave, or laser and microwave only combination groups exhibited a substantial rise in concentrations of MDA relative to the control normal mice. In contrast to the DMBA/croton oil-SKCA-induced control animals, MDA levels were much lower in the IRL, MW, and combination of IRL and MW activated groups when TiO<sub>2</sub>/RB@CSNP was given, but this effect did not reach the level of control normal mice.

#### (TiO<sub>2</sub>/RB@CSNP) PDT, MWDT, MWPDT and the antioxidant system in vivo SKCA models

Figure 8 illustrates how TiO<sub>2</sub>/RB@CSNP, PDT, MWDT, and MWPDT affected the antioxidant indicators (Catalase, SOD, TAC, GR, GPx and GST) in each of the research groups of mice. The DMBA/croton oil-SKCA-induced control group was compared to the TiO<sub>2</sub>/RB@CSNP alone without activation. Only marginally significant alterations were seen in the TAC level, GPx, GST, GR, SOD, and catalase activities. The untreated control DMBA/croton oil-SKCA-induced mice exhibited considerably lower levels of GPx, GST, GR, SOD, Catalase, and TAC than the normal control mice. Furthermore, regarding to the healthy control group of mice, all DMBA/croton oil-SKCA-induced mouse groups treated with laser, microwave, or laser and microwave combination solely exhibited a significant reduction in TAC levels as well as GPx, GST, GR, SOD, and Catalase activities. Activated TiO<sub>2</sub>/RB@CSNP in the IRL, MW, and combination of IRL and MW groups demonstrated a considerable elevation in the TAC level and the activities of Catalase, SOD, GR, GPx, and GST while did not approach the level of normal control group levels, in contrast to the untreated DMBA/croton oil-SKCA-induced control mice.

#### (TiO<sub>2</sub>/RB@CSNP) PDT, MWDT, MWPDT treatment improved liver functions in vivo SKCA models

Figure (9) shows the results of the function liver tests performed on each group under study. While the sera levels of the untreated DMBA/croton oil-SKCA-induced

(See figure on next page.)

**Fig. 4** The effect of different treatment modalities on skin cancer (A-375) cell cycle distribution in all in vitro study groups; 1. Cells were exposed to different treatment modalities for 24 h, 2. Cell cycle distribution was determined using DNA cytometry analysis and different cell phases were plotted as percentage of total events; SubG1(%):  $F = 329.212$   $p < 0.001^*$ , G0/G1(%):  $F = 88.084$   $p < 0.001^*$ , S(%):  $F = 92.935$   $p < 0.001^*$ , G2/M(%):  $F = 173.137$   $p < 0.001^*$ . Mean  $\pm$  SD is used to illustrate the results ( $n = 3$ ). F stands for the ANOVA test value.<sup>abc,de</sup> Significance to (skin cancer untreated group, TiO<sub>2</sub>/RB@CSNP treated non activated group, laser-, microwave-, laser + microwave- exposed groups)

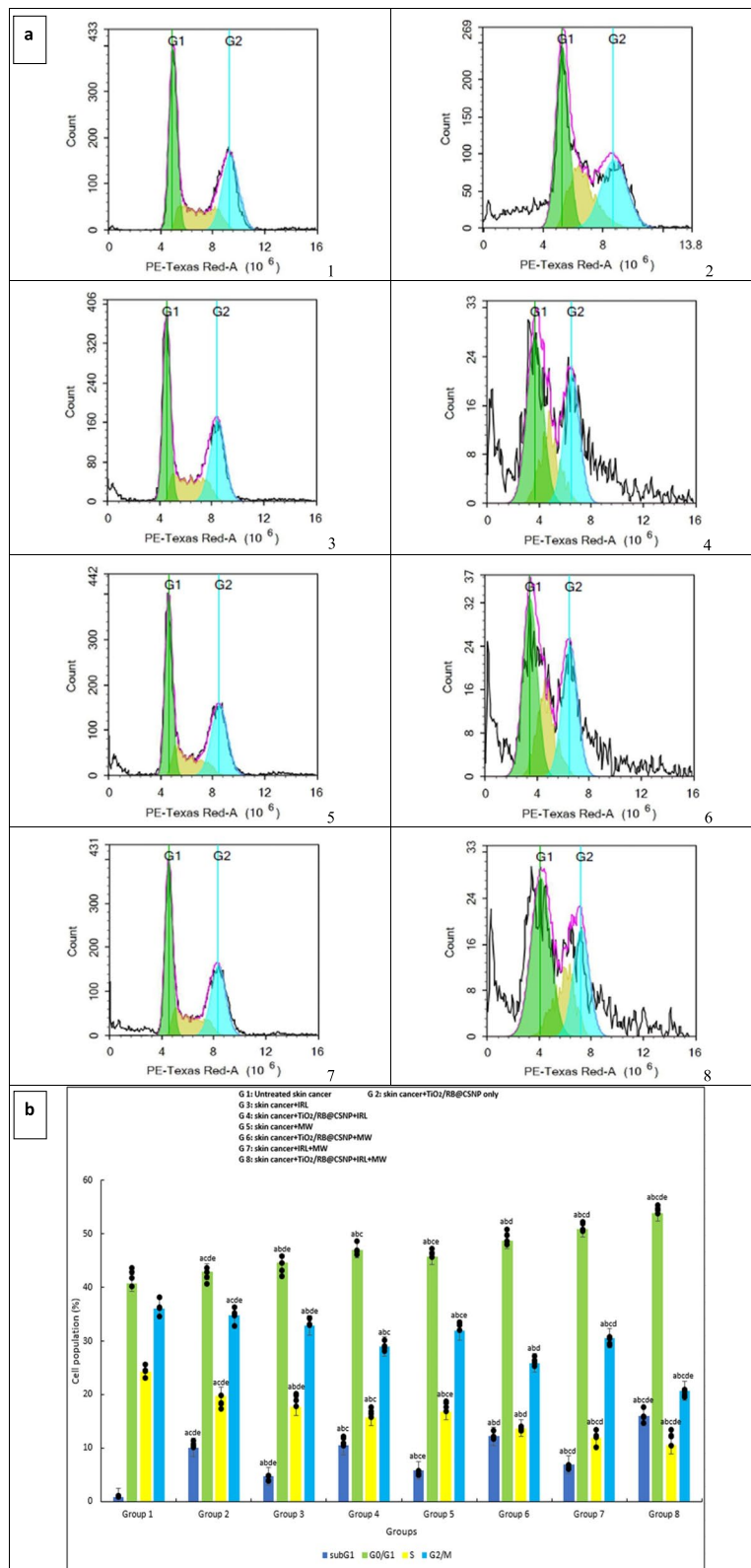


**Fig. 4** (See legend on previous page.)

control group were significantly higher than those in the normal control healthy mice, the levels of AST and ALT in the mice treated with TiO<sub>2</sub>/RB@CSNP alone without irradiation showed only marginally different changes from the untreated DMBA/croton oil-SKCA-induced control group. Furthermore, all DMBA/croton oil-SKCA-induced mice treated with laser, microwave, or of laser and microwave combination only groups displayed a significantly higher of AST and ALT level in comparison to the control normal group. Furthermore, as comparison to the untreated DMBA/croton oil-SKCA-induced control mice, the level of AST and ALT was dramatically reduced when TiO<sub>2</sub>/RB@CSNP was given to the IRL, MW, and combination of IRL and MW activated groups; nevertheless, the normal control group levels was not reached.

#### **(TiO<sub>2</sub>/RB@CSNP) PDT, MWD, MWPDT treatment improved kidney functions in vivo SKCA models**

Figure (9) shows the results of the function kidney tests performed all the groups under study. When compared to the untreated control DMBA/croton oil-SKCA-induced mice, the serum levels of creatinine or urea in mice treated with TiO<sub>2</sub>/RB@CSNP alone without irradiation showed only marginally significant changes; however, this parameter levels in the untreated control DMBA/croton oil-SKCA-induced mice were higher significantly when compared to the control healthy normal mice. Furthermore, all DMBA/croton oil-SKCA-induced mice treated with laser, microwave, or laser and microwave combination only groups showed a statistically significant elevation in creatinine and urea levels relative to the control normal group. Furthermore, when compared to the untreated control DMBA/croton oil-SKCA-induced mice, the administration of TiO<sub>2</sub>/RB@CSNP in the IRL, MW, and combination of IRL and MW activated groups considerably reduced the levels of creatinine and urea; however, the normal control group levels was not reached.

#### **(TiO<sub>2</sub>/RB@CSNP) PDT, MWD, MWPDT anticancer, antiproliferative and antiangiogenic effects in vivo SKCA models**

Figure 10 shows the effects of TiO<sub>2</sub>/RB@CSNP on the genes relative expressions of VEGF, TNF alpha, Bax,

Caspase (3, 9), Bcl-2, and p53 in all groups under study. When TiO<sub>2</sub>/RB@CSNP was administered to mice in isolation without activation, the expression of VEGF, TNF alpha, Bax, Caspase (3, 9), Bcl-2, and p53 changed only slightly in comparison to the untreated control DMBA/croton oil-SKCA-induced group. In contrast, the untreated control DMBA/croton oil-SKCA-induced group's levels of caspase (3, 9), TNF alpha, Bax, and p53 were declined significantly, while those of Bcl-2, and VEGF were elevated significantly than those of control normal, healthy mice. Furthermore, regarding to the healthy control group of mice, all DMBA/croton oil-SKCA-induced mice treated with laser, microwave, or laser and microwave combination only groups exhibited significantly elevated levels of VEGF and Bcl-2 gene expressions and significantly decreased levels of TNF alpha, caspase (3, 9), Bax, and p53 gene expressions. The delivery of TiO<sub>2</sub>/RB@CSNP to the IRL, MW, and combination of IRL and MW activated groups resulted in significant increases in the TNF alpha, caspase (3, 9), Bax, and p53 genes expressions, and significant decreases in the expressions of the genes VEGF and Bcl-2, as compared to the control untreated DMBA/croton oil-SKCA-induced group.

#### **(TiO<sub>2</sub>/RB@CSNP) PDT, MWD, MWPDT histopathological effect on in vivo SKCA models**

Figure (11) displays the H&E stained tissue sections from all study mouse groups that demonstrate how TiO<sub>2</sub>/RB@CSNP, PDT, MWD, and MWPDT affect SKCA caused by DMBA/croton oil. According to the histological study, all of the tumors in the untreated control DMBA/croton oil-SKCA-induced group exhibited 5% necrosis and were completely composed of extremely malignant cells. In comparison to the untreated control DMBA/croton oil-SKCA-induced mice, the histologically induced SKCA tissues showed only marginally significant alterations in the mice treated with TiO<sub>2</sub>/RB@CSNP alone, without irradiation. The administration of TiO<sub>2</sub>/RB@CSNP in the laser, microwave, and laser and microwave combination activated groups showed significantly necrotic large foci areas (85–90%) in regards to the untreated control DMBA/croton oil-SKCA-induced mice. Additionally, all DMBA/croton oil-SKCA-induced mice treated with IRL,

(See figure on next page.)

**Fig. 5** The effect of different treatment modalities on skin cancer (A-375) apoptosis and necrosis in all in vitro study groups; 1. Cells were exposed to different treatment modalities for 24 h, 2. Cells were stained with annexin V-FITC/PI and different cell populations were plotted as percentage of total events. early apoptosis (%):  $F = 16.884$   $p < 0.001^*$ , late apoptosis (%):  $F = 26.304$   $p < 0.001^*$ , early and late apoptosis (%):  $F = 23.439$   $p < 0.001^*$ , necrosis (%):  $F = 18.719$   $p < 0.001^*$ , total cell death (%):  $F = 23.288$   $p < 0.001^*$ . Mean  $\pm$  SD is used to illustrate the results ( $n = 3$ ). F stands for the ANOVA test value. <sup>a,b,c,d,e</sup> Significance to (skin cancer untreated group, TiO<sub>2</sub>/RB@CSNP treated non activated group, laser-, microwave-, laser + microwave- exposed groups)

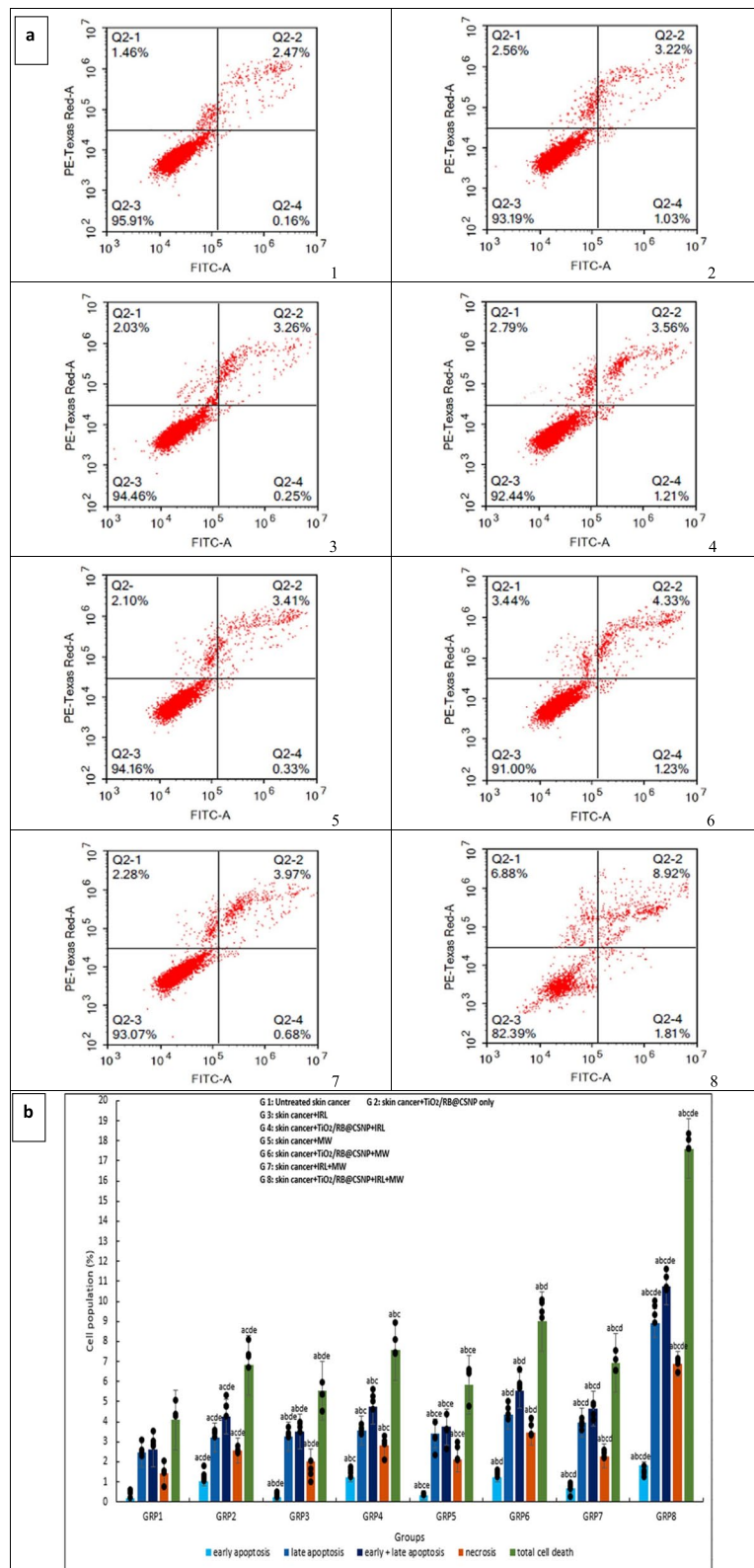


**Fig. 5** (See legend on previous page.)

MW, or IRL and MW combination only showed considerable areas of necrosis regarding to the untreated control DMBA/croton oil-SKCA-induced group.

## Discussion

Skin cancer is now the sixth most prevalent malignancy worldwide to be reported, which has an impact on both the economic and global health. The statistics on SKCA have been further worsened by industrialization, genetic manipulation, and the rapidly increasing environmental changes. The cost, toxicity, and bioavailability of several current treatment modalities, including surgery, radiation, conventional chemotherapy and immunotherapy, are causing a loss in their efficacy in treating SKCA and a decrease in patient compliance. To date, there have been a number of Nano-technological developments that have helped to overcome this constraint. Of all the nanomaterials, nanoparticles have provided enormous benefits by serving as medication carriers and therapeutic agents for the amazing treatment of SKCA. Because of their tiny size and high surface area to volume ratio, targeted therapy with nanoparticles increases the uptake of SKCA through their leaky vasculature, which improves therapeutic efficacy [1, 5, 6, 34–36].

The results of SRB assay is a valuable test that measures viable cell count precisely and evaluates the cytotoxicity of drugs used in cancer treatment. Additionally, one of the most important mechanisms causing cancer is the disruption of the cell cycle that is the basic process which governs a cell's life activities. Moreover, three forms of programmed cell death that counteract biological processes of proliferation and are essential to appropriate development are apoptosis, necrosis, and autophagy. Since most malignancies require tumor cells to have the ability to overpower apoptosis in order to survive, it is thought that the formation and growth of tumors are related to blocked apoptosis and aberrant proliferation [37–40].

The findings of the SRB assay (cytotoxicity) and flow cytometer (cell cycle analysis, apoptosis, necrosis, and autophagy) in this study showed that there was only a minor impact on the SKCA-A-375 cell line following a 24-h incubation period and treatment with TiO<sub>2</sub>/RB@CSNP without activation. The SKCA-A-375 cell line is not significantly affected by the application of laser

and shockwave in the absence of TiO<sub>2</sub>/RB@CSNP. The effectiveness of the microwave (MWDT) and the laser (PDT) is increased when TiO<sub>2</sub>/RB@CSNP is present. The obtained results demonstrated that the combined therapeutic method (MWPDT) is more effective than either IRL or MW alone in treating the SKCA-A-375 cell line (cell viability decreased in a dose-responsive manner, the cell cycle progression in G<sub>0</sub>/G<sub>1</sub> was slowed down, and cell death was induced as evidenced by an increase in the population of Pre-G cells, an increase in early and late apoptosis and necrosis, and an increase in autophagic cell death). Our findings are consistent with prior research [41–45], that demonstrated that the sensitizer TiO<sub>2</sub>/RB@CSNP with both MW (-Micro) and IRL (-photo) combined activation (MWPDT) had the greatest inhibitory effect (cell cycle arrest; progression decline of cell cycle in G<sub>0</sub>/G<sub>1</sub> phase) and destroyed tumor cells (in a dose-dependent manner, reduction cell viability, increasing apoptosis, necrosis, and autophagy). This was followed by TiO<sub>2</sub>/RB@CSNP-MW and IRL activation alone (MWDT and PDT), with MWPDT more effective than MWDT and PDT.

7,12-dimethylbenz[a]-anthracene (DMBA) is a compelling skin carcinogen that increases the occurrence of SKCA, along with the use of SKCA promoters like croton oil. SKCA spreads in three phases: initiation, promotion, and progression. DMBA causes SKCA through various processes, including the formation of dihydrodiol-epoxide (carcinogen) or 1,2-epoxide-3,4-diol DMBA by cytochrome P450 family 1 subfamily A, B member 1 (CYP1 A1, CYP1B1) and cytochrome P450 enzyme (CYP450). This leads to the formation of deoxyribose nucleic acid (DNA) adducts. The ultimate carcinogen that mediates carcinogenesis causes oxidative DNA damage, chronic inflammation, and reactive oxygen species (ROS) overproduction, which in turn causes mutations necessary for tumor formation [46–48].

The current investigation offers proof of the oxidants that the DMBA/croton oil-induced SKCA is advancing. The MDA levels in the untreated DMBA/croton oil-SKCA-induced control mice were significantly higher. Regarding to untreated DMBA/croton oil-SKCA-induced control mice, MDA levels were considerably reduced in all TiO<sub>2</sub>/RB@CSNP treated groups (non irradiated, laser-activated, microwave-activated, and combination of

(See figure on next page.)

**Fig. 6** The effect of different treatment modalities on skin cancer (A-375) autophagy in all in vitro study groups; 1. Cells were exposed to different treatment modalities for 24 h; and were stained with Cyto-ID autophagosome tracker. 2. Net fluorescent intensity (NFI; red color) were plotted and compared to basal fluorescence of control group (green color). autophagy (%):  $F = 24.876$   $p < 0.001^*$ . Mean  $\pm$  SD is used to illustrate the results ( $n = 3$ ). F stands for the ANOVA test value. <sup>a,b,c,d,e</sup> Significance to (skin cancer untreated group, TiO<sub>2</sub>/RB@CSNP treated non activated group, laser-, microwave-, laser + microwave- exposed groups)

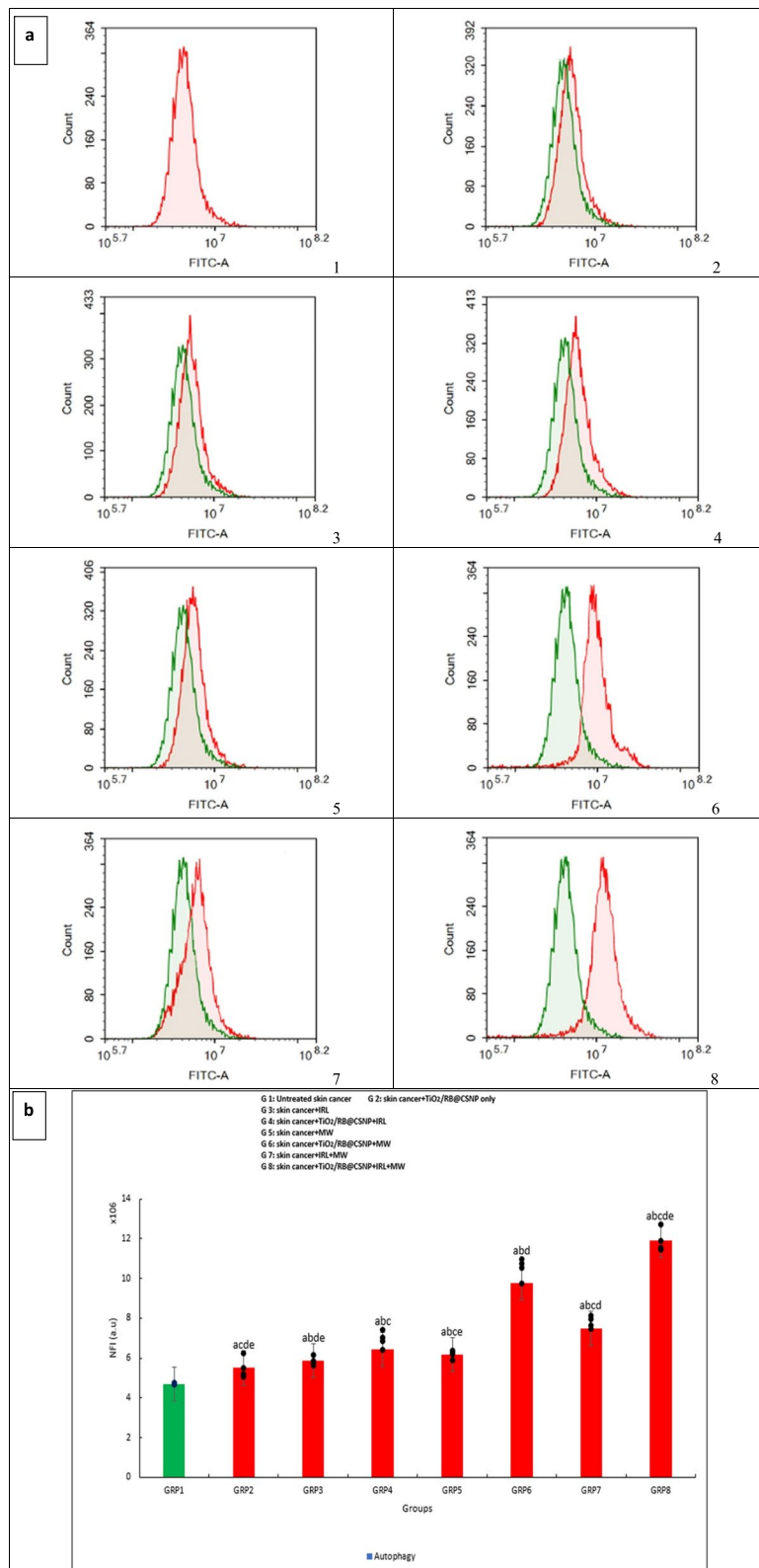


**Fig. 6** (See legend on previous page.)

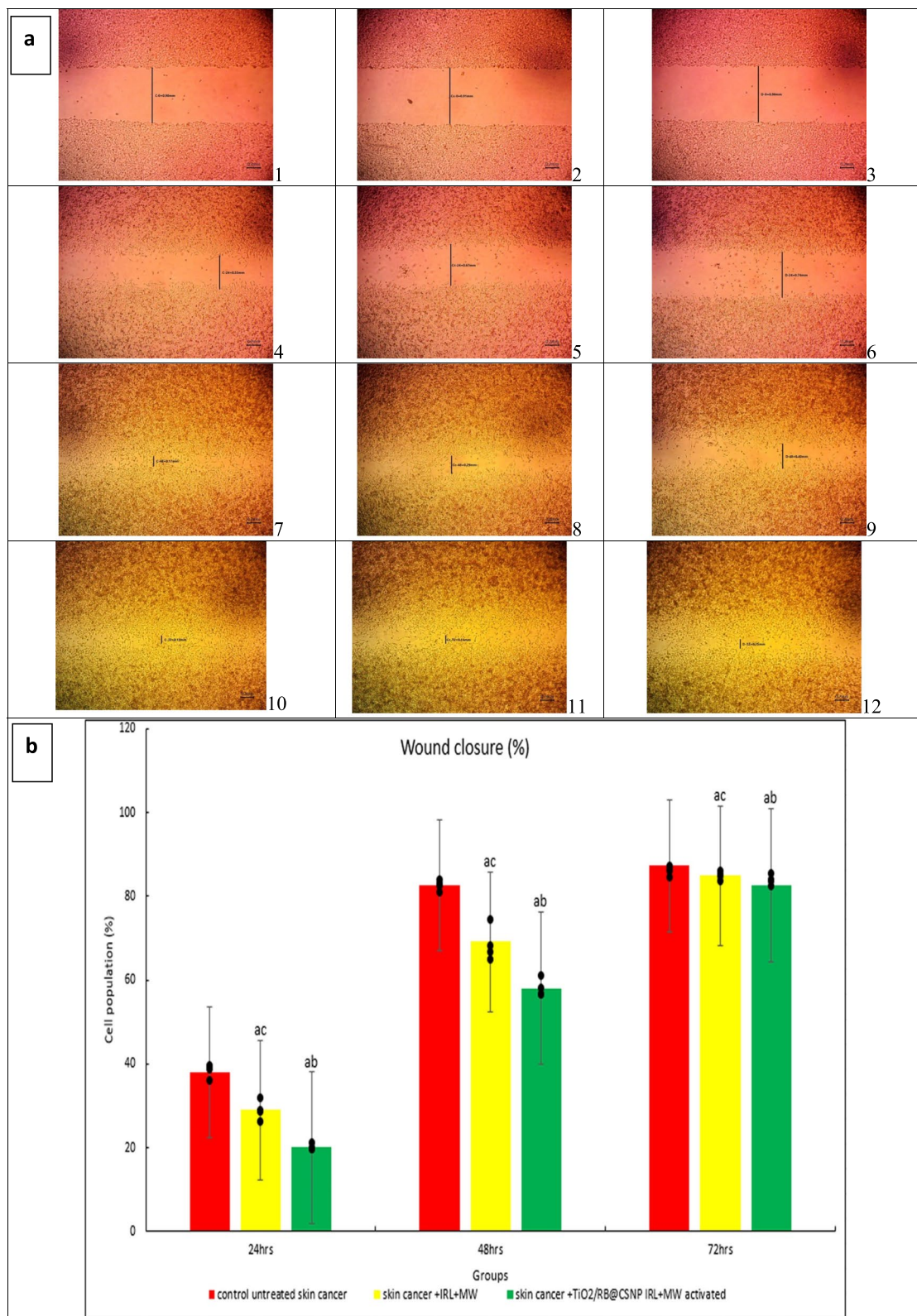


**Fig. 7** The effect of different treatment modalities on skin cancer (A-375) migration; 1. A-375 untreated, 2. A-375 treated with laser + microwave only, 3. A-375 treated with TiO<sub>2</sub>/RB@CSNP + laser + microwave. wound closure-24 h (%):  $F = 2.416E3$   $p < 0.001^*$ , wound closure-48 h (%):  $F = 694.712$   $p < 0.001^*$ , wound closure-72 h (%):  $F = 2.855E3$   $p < 0.001^*$ . Mean  $\pm$  SD is used to illustrate the results ( $n = 3$ ). F stands for the ANOVA test value. <sup>a,b,c</sup> Significance to (skin cancer untreated group, laser + microwave only group, laser + microwave + TiO<sub>2</sub>/RB@CSNP groups)

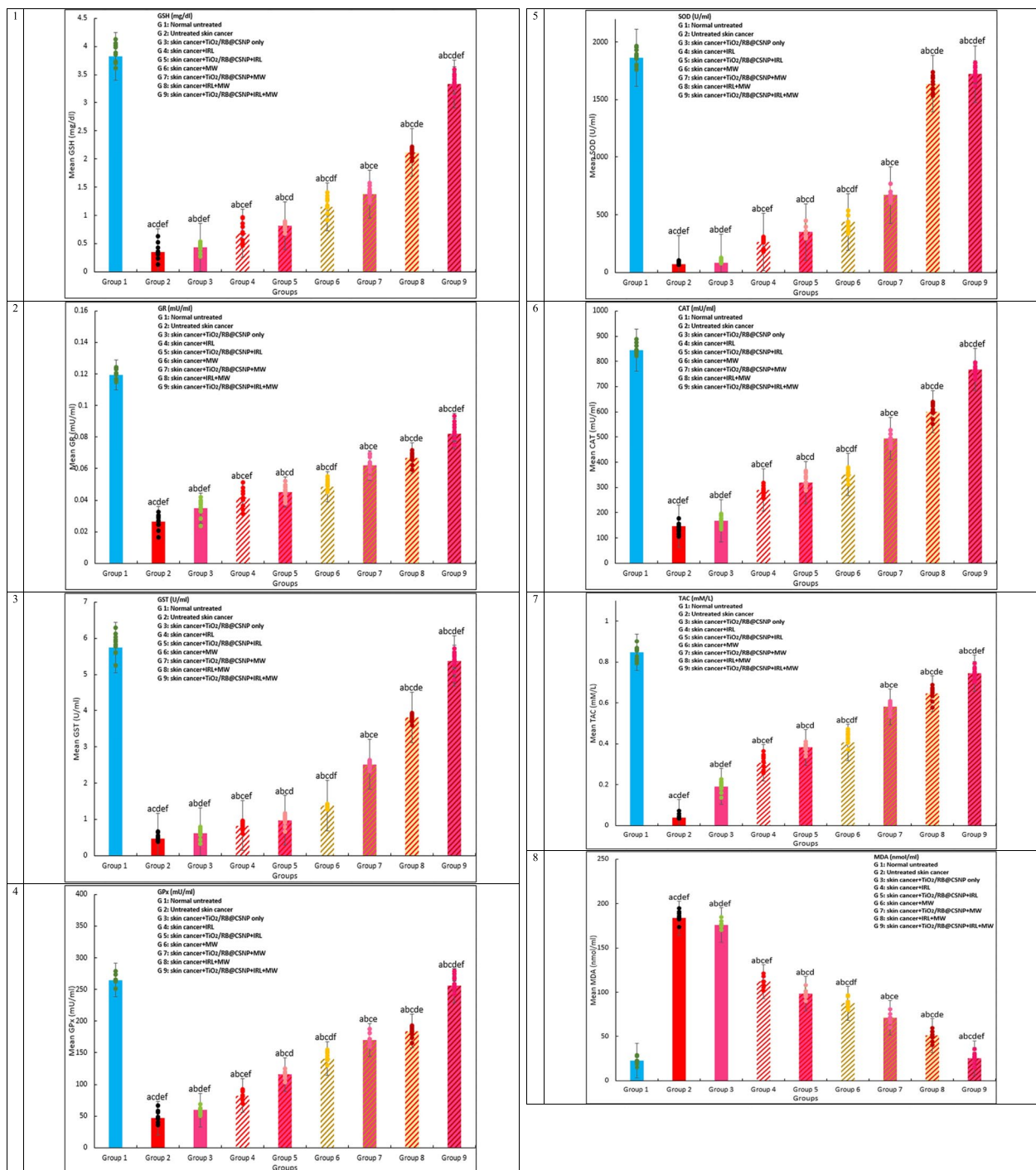


**Fig. 8** The effect of different treatment modalities on MDA, antioxidants activities, and capacities in all study groups; F: value for ANOVA test 1. GSH(mg/dl):  $F = 871.530 p < 0.001^*$ , 2. GR (mU/ml):  $F = 161.065 p < 0.001^*$ , 3. GST (U/ml):  $F = 1.221E3 p < 0.001^*$ , 4. GPx (mU/ml):  $F = 4.155E4 p < 0.001^*$ , 5. SOD (U/ml):  $F = 3.819E6 p < 0.001^*$ , 6. CAT(mU/ml):  $F = 1.676E5 p < 0.001^*$ , 7. TAC(mM/L):  $F = 453.839 p < 0.001^*$ , 8. MDA(nmol/ml):  $F = 9.736E4 p < 0.001^*$ . Mean  $\pm$  SD is used to illustrate the results ( $n = 10$ ). F stands for the ANOVA test value..<sup>a,b,c,d,e</sup> Significance to (skin cancer untreated group, TiO<sub>2</sub>/RB@CSNP treated non activated group, laser-, microwave-, laser + microwave- exposed groups)

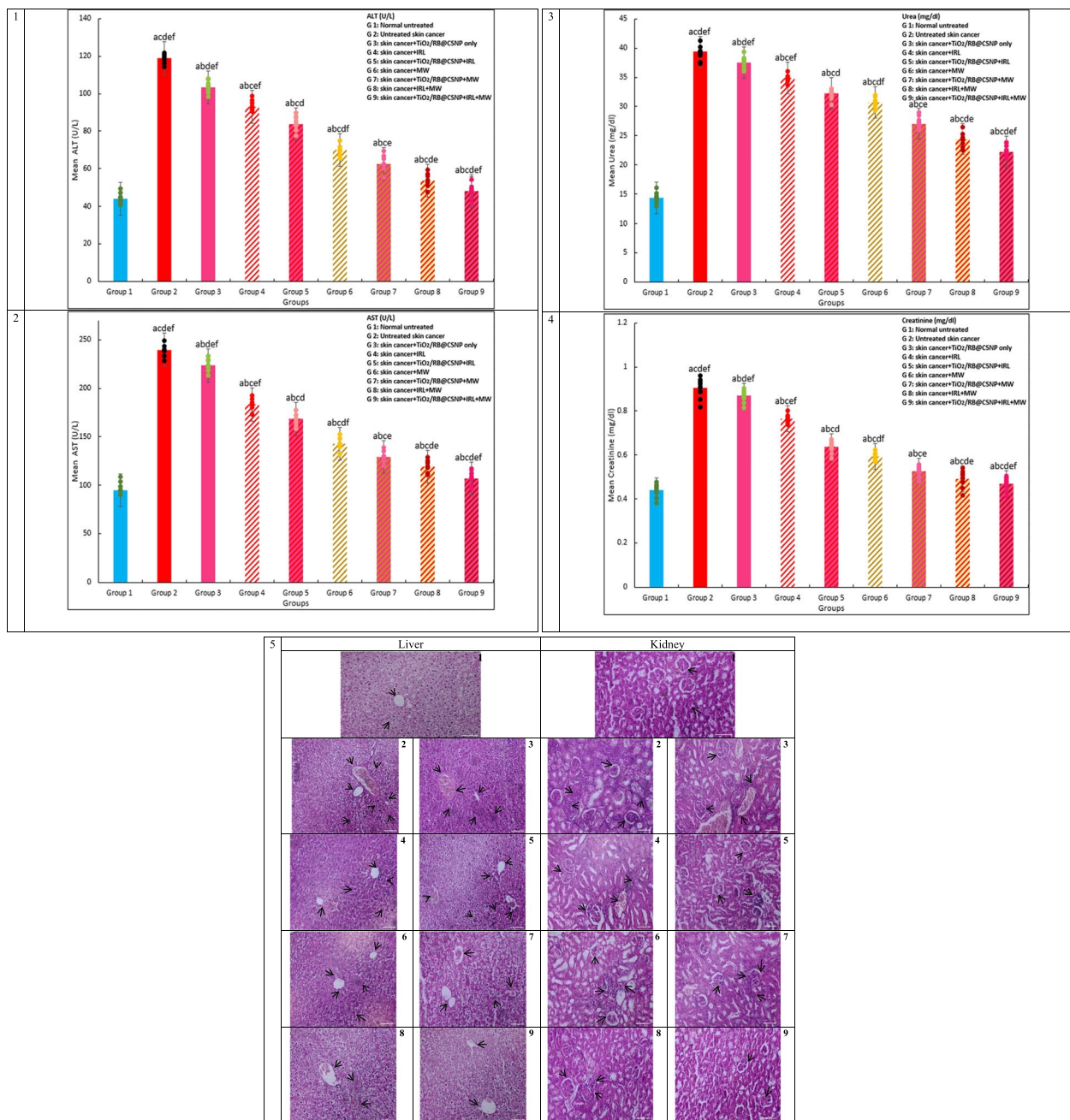


**Fig. 9** The effect of different treatment modalities on hepatic, renal biomarkers biomarkers and tissues histopathology in all study groups; F: value for ANOVA test 1. ALT (U/L):  $F = 7.865E3$   $p < 0.001^*$ , 2. AST (U/L):  $F = 1.651E5$   $p < 0.001^*$ , 3. Urea (mg/dl):  $F = 4.230E3$   $p < 0.001^*$ , 4. Creatinine (mg/dl):  $F = 401.771$   $p < 0.001^*$ . 5. H&E stained liver and kidney tissues; (1. Normal untreated group, 2. DMBA/croton oil induced SKCA group without any treatment, 3. DMBA/croton oil induced SKCA group treated with  $TiO_2/RB@CSNP$  without activation, 4. DMBA/croton oil SKCA induced group subjected to laser only, 5. DMBA/croton oil SKCA induced group subjected to laser in  $TiO_2/RB@CSNP$  presence, 6. DMBA/croton oil induced SKCA group subjected to microwave only, 7. DMBA/croton oil SKCA induced group subjected to microwave in  $TiO_2/RB@CSNP$  presence, 8. DMBA/croton oil SKCA induced group subjected to combined modalities laser/microwave only, 9. DMBA/croton oil SKCA induced group subjected to combined modalities laser/microwave in  $TiO_2/RB@CSNP$  presence. Mean  $\pm$  SD is used to illustrate the results ( $n = 10$ ). F stands for the ANOVA test value. <sup>a,b,c,d,e</sup> Significance to (skin cancer untreated group,  $TiO_2/RB@CSNP$  treated non activated group, laser-, microwave-, laser + microwave- exposed groups)

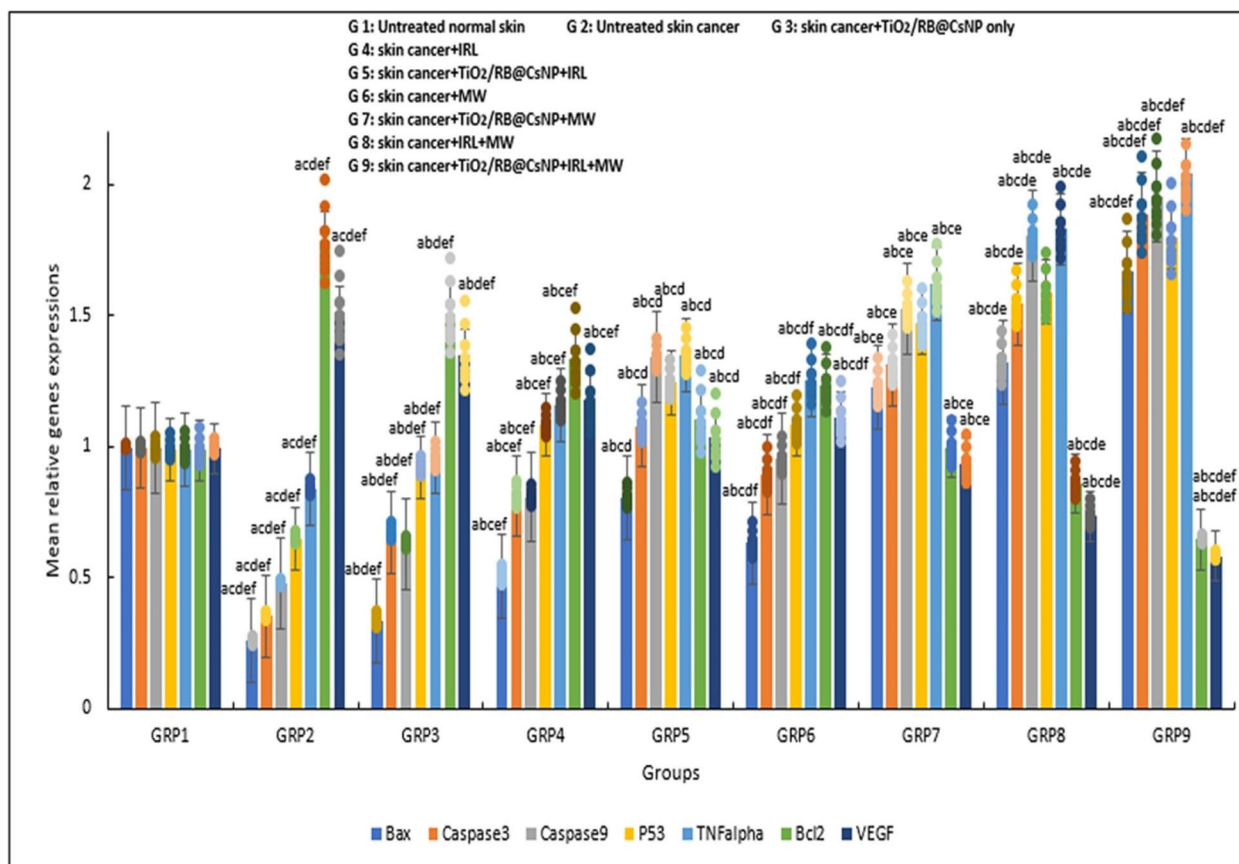


**Fig. 10** The effect of different treatment modalities on VEGF, TNF alpha, Bax, Caspase (9,3), Bcl-2 and p53, qRT-PCR relative genes expressions in all study groups; F: value for ANOVA test. p53:  $F = 406.566 p < 0.001^*$ , Bax:  $F = 985.443 p < 0.001^*$ , Caspase 9:  $F = 1.053E3 p < 0.001^*$ , Caspase 3:  $F = 761.080 p < 0.001^*$ , TNFalpha:  $F = 435.687 p < 0.001^*$ , VEGF:  $F = 147.444 p < 0.001^*$ , Bcl-2:  $F = 191.970 p < 0.001^*$ . Mean  $\pm$ SD is used to illustrate the results ( $n = 10$ ). F stands for the ANOVA test value. <sup>a,b,c,d,e</sup> Significance to (skin cancer untreated group, TiO<sub>2</sub>/RB@CSNP treated non activated group, laser-, microwave-, laser + microwave- exposed groups)

laser and microwave-activated mice). Significant reductions in the TAC backup and in the activities of Catalase, GST, GPx, GR, and SOD further disrupt the antioxidant system. The antioxidant levels in the DMBA/croton oil-SKCA-induced control mice which were not treated were significantly lower. Antioxidant levels were considerably higher in all TiO<sub>2</sub>/RB@CSNP treated groups (laser-activated, microwave-activated, and combination of laser and microwave-activated) than in untreated control DMBA/croton oil-SKCA-induced mice. Previous studies have shown that induction of DMBA/croton oil SKCA

results in a rise in MDA significantly and a decline in TAC, and Catalase, GST, GPx, GR, SOD activities [49–54]. It was discovered that mice with SKCA generated by DMBA/croton oil showed reduced activity in scavenging free radicals and were more vulnerable to lipid peroxidation than mice from healthy normal control. As previously mentioned, DMBA/croton oil-SKCA-induction promotes the generation of various free radical metabolites, leading to an excess and accumulation of ROS as well as an increase in the oxidation of cell phospholipid polyunsaturated fatty acid bilayers, which in turn raises

(See figure on next page.)

**Fig. 11** The in vivo study groups images and H&E skin tissue stained section demonstrating the effect of different treatment modalities on cellular level in all study groups; 1. Normal untreated group, 2. DMBA/croton oil induced SKCA group without any treatment, 3. TiO<sub>2</sub>/RB@CSNP treated group without activation, 4. DMBA/croton oil SKCA induced group subjected to laser only, 5. DMBA/croton oil SKCA induced group subjected to laser in presence of TiO<sub>2</sub>/RB@CSNP, 6. DMBA/croton oil induced SKCA group subjected to microwave only, 7. DMBA/croton oil SKCA induced group subjected to microwave in presence of TiO<sub>2</sub>/RB@CSNP, 8. DMBA/croton oil SKCA induced group subjected to combined modalities laser/microwave only, 9. DMBA/croton oil SKCA induced group subjected to combined modalities laser/microwave in presence of TiO<sub>2</sub>/RB@CSNP

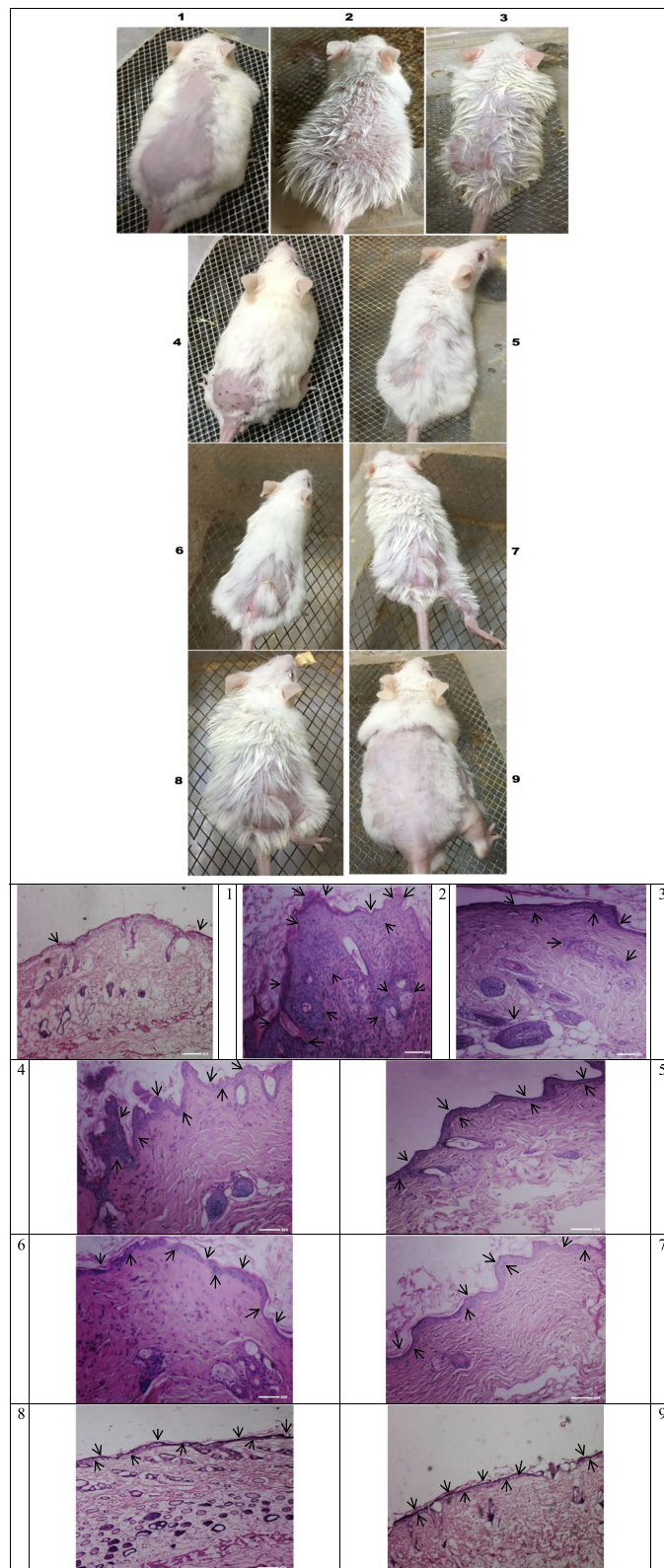


**Fig. 11** (See legend on previous page.)

MDA levels. The deterioration of enzymatic and non-enzymatic antioxidants is a critical step in the oxidative stress development and cancer evolve. These antioxidants, both enzymatic and non-enzymatic, were continuously depleted, which explained why they were needed to detoxify DMBA/croton oil-SKCA-induced ROS and their metabolites, which explained why they were lacking. The accumulation of ROS may compromise the catalytic activity of enzymatic antioxidants [48–54]. Our findings demonstrated how the anti-lipid peroxidative action of non activated part of TiO<sub>2</sub>/RB@CSNP is supported by its ability to scavenge free radical generation decreasing MDA levels. Furthermore shows the effectiveness of TiO<sub>2</sub>/RB@CSNP as MWPS and its action upon activation by PDT, MWDT, and MWPD, which eliminated DMBA/croton oil-SKCA cancerous cells; the primary ROS source, causing a restoration and rise in antioxidant enzyme activities and restrict the depletion of antioxidant system and a transition from a cancerous state to a state that is almost normal. Our results agreed with previous studies [55–63] reported the biochemical MWPD impact (restoration of enzymatic and non-enzymatic antioxidants to near normal levels, reduction of MDA levels, and destruction of DMBA/croton oil-SKCA cells, the fundamental root cause of ROS, and prevention of antioxidant exhaustion by ROS generated from DMBA/croton oil-SKCA-induced cells) was greatest when TiO<sub>2</sub>/RB@CSNP was present as a MWPS in conjunction with both MW (-Micro) and IRL (-photo) activation, followed by TiO<sub>2</sub>/RB@CSNP-MW and IRL activation alone.

In the DMBA/croton oil-SKCA-induced groups in our investigation; there was a substantial increase in ALT and AST, suggesting liver cell damage. Elevated levels of several liver enzymes in serum are associated with cellular leakage of those enzymes into the bloodstream, which is indicative of damage to the hepatocyte's integrity in the cell membrane. Because DMBA/croton oil disrupts metabolism and induces organ failure, the results of the present study are in line with previous studies in showing that hepatic function was reduced in DMBA/croton oil-SKCA-induced animals regarding to control normal mice [46–52, 64–72]. The current study discovered that TiO<sub>2</sub>/RB@CSNP decreased ALT and AST levels, indicating liver protection. Furthermore, this bolsters the protective efficacy of TiO<sub>2</sub>/RB@CSNP in averting hepatic-dysfunction in mice induced by DMBA/croton oil-SKCA. Additionally, DMBA/croton oil triggered a clear elevation in creatinine and urea in the DMBA/croton oil-SKCA-induced groups in this study, indicating renal damage. It has been demonstrated that cardiac and hepatic damage causes renal dysfunction in DMBA/croton oil-SKCA-induced mice, resulting in increased tubular and glomerular congestion. Due to this congestion, results in renal

interstitial pressure increase over the entire capillary and tubule system. The findings of this investigation support previous findings by showing that, compared to control normal mice, DMBA/croton oil-SKCA-induced mice had decreased renal function [48–54, 64–72]. The current study discovered that TiO<sub>2</sub>/RB@CSNP decreased serum levels of creatinine and urea, which evoke kidney protection. Moreover, this validates the preventative activity of TiO<sub>2</sub>/RB@CSNP in averting renal impairment in mice that is induced by DMBA/croton oil-SKCA. Our findings demonstrated that the non-activated component of TiO<sub>2</sub>/RB@CSNP scavenges free radicals generated by DMBA/croton oil-SKCA induction, protecting the liver and kidneys. Furthermore, DMBA/croton oil, the primary cause of ROS, is efficiently eliminated by activated TiO<sub>2</sub>/RB@CSNP, which results in the recovery of liver and kidney function as well as transition from a malignant to a condition that is almost normal. The MWPD was superior to MWDT and PDT, and the ameliorating impact was greatest when TiO<sub>2</sub>/RB@CSNP was present as a MWPS in combination with both MW (-Micro) and IRL (-photo) activation, followed by TiO<sub>2</sub>/RB@CSNP-mw and IRL activation only.

The expressions of TNF alpha, Caspase (3,9), p53, Bcl-2, Bax, and VEGF were molecularly assessed in the current study as indicators of DMBA/croton oil-induced SKCA treatment and inhibition of angiogenesis, respectively. The results indicate a significant negative correlation between the gene expressions and DMBA/croton oil-SKCA-induction, but a positive marked correlation between treatment with different modalities in the presence of TiO<sub>2</sub>/RB@CSNP and the gene expressions. The MWPD with (TiO<sub>2</sub>/RB@CSNP) treated mice groups had significantly higher expression of the genes TNF alpha, caspase 3, 9, Bax, p53 than did the PDT or MWDT with (TiO<sub>2</sub>/RB@CSNP), IRL or MW only without (TiO<sub>2</sub>/RB@CSNP), and the untreated DMBA/croton oil-SKCA-induced mice. On the other hand, in the untreated DMBA/croton oil-SKCA-induced animals, there was a positive association between Bcl-2 and VEGF expressions, whereas in the TiO<sub>2</sub>/RB@CSNP presence, there was a negative correlation between treatment modalities with VEGF and Bcl-2 expressions. Compared to mice subjected to PDT or MWDT with (TiO<sub>2</sub>/RB@CSNP) alone, and then IRL or MW alone without (TiO<sub>2</sub>/RB@CSNP) alone, the expressions of the VEGF and Bcl-2 genes were considerably lower in mice subjected to MWPD with (TiO<sub>2</sub>/RB@CSNP). In DMBA/croton oil stimulated SKCA untreated mice group, the expression was highest. Our study's results, which are consistent with those of other studies, show that expressions of TNF alpha, Caspase (3,9), Bax, p53, VEGF and Bcl-2 genes as a reliable indicators of

cancer-relevant treatment [32, 72–76]. demonstrating the MWPDT implications on molecular level (VEGF and Bcl-2 genes down regulation; limiting the angiogenesis capabilities and restricting the proliferation of DMBA/croton oil-induced SKCA cells) and (TNF alpha, Bax, p53, and caspase 3, 9 pro-apoptotic genes up regulation; directing DMBA/croton oil-induced SKCA cells to be eradicated by either necrosis or apoptosis and promoting the immune system). Additionally, MWPDT was superior to MWDT and PDT when TiO<sub>2</sub>/RB@CSNP was used as a MWPS in combination with both MW (-Micro) and IRL (-photo) activation.

Current study indicated that TiO<sub>2</sub>/RB@CSNP could be used as a micro- and photo- sensitizer to cure in vivo SKCA caused by DMBA/croton oil. The TiO<sub>2</sub>/RB@CSNP significantly reduces cancer and causes cell death. It can be triggered by chemical activation mechanisms that are mediated by photons or microwave. The biological impact of MWPDT may be elaborated by micro-photochemical/physical mechanisms, such as the excitation of a ground state MWPS (TiO<sub>2</sub>/RB@CSNP) molecule in a singlet state by laser light and microwave, which propels an electron into a higher energy orbital. The MWPS excited triplet state has a comparatively long half-life (~ microseconds) at lower energies until internal or fluorescence conversion returns it to the ground state (~ nanoseconds). On the other hand, the spin of the excited electron inverts. Phosphorescence loses its excitation energy and to the ground singlet state returns in a spin-forbidden transfer. Triplet oxygen excitation can either transfer an electron to superoxide anions, which can produce a variety of ROS that can seriously harm biological systems, or it can transfer its energy to triplet molecular oxygen, which can produce reactive physiologically stimulated singlet state oxygen that can cause serious harm to biological systems. Both the innate and adaptive immune systems respond to MWPDT with a robust defense. Additionally, it kills cells by a variety of mechanisms, including apoptosis, autophagy, and necrosis.

As of this moment, our research indicates that TiO<sub>2</sub>/RB@CSNP may be used as a photo- and microwave sensitizer to cure in vivo SKCA caused by DMBA/croton oil. The TiO<sub>2</sub>/RB@CSNP significantly inhibits tumor growth and causes cell death, which may be triggered by chemical activation processes mediated by photons or microwave. Anticancer effects can be obtained by using microwave and laser in TiO<sub>2</sub>/RB@CSNP presence. It is suggested that light photon dynamic therapy in conjunction with microwave dynamic therapy is a very effective anticancer treatment. Based on our research, TiO<sub>2</sub>/RB@CSNP shows great promise as a novel sensitizer and as a helpful drug delivery system for micro-photodynamic therapy (MWPDT).

## Conclusion

The application of titanium dioxide and rose bengal conjugated chitosan nanoparticles (TiO<sub>2</sub>/RB@CSNP) as a sensitizer delivery system for micro-photodynamic treatment (MWPDT) of skin cancer in vitro (using the A-375 cell line) and in vivo (using DMBA/croton oil-induced mice) demonstrated significant results in this work, indicating promising outcomes in the treatment of cancer. In addition, TiO<sub>2</sub>/RB@CSNP's many benefits, including its low systemic toxicity and excellent bioavailability, make it a feasible alternative for treating cancer. Moreover, the combination of TiO<sub>2</sub>/RB@CSNP@IRL@MW has opened up a wide range of options for anticancer drugs for the effective eradication of skin cancer.

## Recommendation

The current study demonstrated the potential of titanium dioxide and rose bengal conjugated chitosan nanoparticles (TiO<sub>2</sub>/RB@CSNP) as a novel sensitizer in conjunction with micro-photodynamic therapy (MWPDT), a therapeutic approach that is still needs more confirmation and further validation for the treatment of skin cancer. It is strongly advised to conduct additional research using techniques that safely apply this cutting-edge approach and technology to people and monitor modifications in various biophysical and/or biochemical indicators.

## Abbreviations

ALT	Alanine aminotransferase
AST	Aspartate aminotransferase
CAT	Catalase
DMBA	7,12-Dimethylbenz[a]anthracene
GPx	Glutathione peroxidase
GR	Glutathione reductase
GSH	Reduced glutathione
GST	Glutathione-S-transferase
MDA	Malondialdehyde
MWDT	Microwave-dynamic treatment
MWPDT	Micro-photo-dynamic therapy
PDT	Photodynamic therapy
ROS	Reactive oxygen species
SKCA	Skin cancer
SOD	Superoxide dismutase
SRB	Sulforhodamine B
TAC	Total antioxidant capacity
TiO <sub>2</sub> /RB@CSNP	Titanium Dioxide / Rose Bengal conjugated chitosan nanoparticles

## Acknowledgements

Not Applicable.

## Authors' contributions

"All authors contributed to the writing of this manuscript, and all contributors approved the final version of the manuscript. S.A.A.E. design the work and wrote the main manuscript text, N.A.M.H. prepared figures, H.S.A.S. participated in interpretation of results, M.A.S.A. participated in statistical analysis, A.M.K. participated in result analysis interpretation and writing, S.M.E.K. participated in discussion writing. All authors reviewed the manuscript."

## Funding

Open access funding provided by The Science, Technology & Innovation Funding Authority (STDF) in cooperation with The Egyptian Knowledge Bank (EKB). This research received no grant from any funding agency.

## Data availability

All data generated or analyzed during this study are included in this published article [and its supplementary information files].

## Declarations

### Ethics approval and consent to participate

Experimental procedures, animal handling and sampling followed the Guide for the Care and Use of Laboratory Animals and were approved by Research Ethical Committee [Institutional Animal Care and Use Committee, (ALEXU-IACUC; Code No.01219112821)] of the Medical Research Institute, Alexandria University (Alexandria, Egypt).

### Consent for publication

Not Applicable.

### Competing interests

The authors declare no competing interests.

### Author details

<sup>1</sup>Applied Medical Chemistry Department, Medical Research Institute, Alexandria University, Alexandria, Egypt. <sup>2</sup>Medical Biophysics Department, Medical Research Institute, Alexandria University, Alexandria, Egypt. <sup>3</sup>Chemistry Department, Faculty of Science, Tanta University, Tanta, Egypt.

Received: 28 July 2024 Accepted: 7 May 2025

Published online: 19 May 2025

## References

- Hasan N, Nadaf A, Imran M, Jiba U, Sheikh A, Almalki WH, et al. Skin cancer: understanding the journey of transformation from conventional to advanced treatment approaches. *Mol Cancer*. 2023;22:168.
- Leiter U, Keim U, Garbe C. Epidemiology of skin cancer: update 2019. *Adv Exp Med Biol*. 2020;1268:123–39.
- Sung H, Ferlay J, Siegel RL, Laversanne M, Soerjomataram I, Jemal A, et al. Global Cancer Statistics 2020: GLOBOCAN estimates of incidence and mortality worldwide for 36 cancers in 185 countries. *CA Cancer J Clin*. 2021;71:209–49.
- Siegel RL, Miller KD, Fuchs HE, Jemal A. Cancer statistics, 2021. *CA Cancer J Clin*. 2021;71:7–33.
- Chandra J, Hasan N, Nasir N, Wahab S, Thanikachalam PV, Sahebkar A, et al. Nanotechnology-empowered strategies in treatment of skin cancer. *Environ Res*. 2023;235:116649.
- Chinembiri TN, du Plessis LH, Gerber M, Hamman JH, du Plessis J. Review of natural compounds for potential skin cancer treatment. *Molecules*. 2014;19:11679–721.
- Sujai PT, Joseph MM, Karunakaran V, Saranya G, Adukkadan RN, Shamjith S, et al. Biogenic cluster-encased gold nanorods as a targeted three-in-one theranostic nanoenvelope for SERS-guided photochemotherapy against metastatic melanoma. *ACS Appl Bio Mater*. 2019;2:588–600.
- Narayanan N, Kim JH, Santhakumar H, Joseph MM, Karunakaran V, Shamjith S, et al. Nanotheranostic probe built on methylene blue loaded cucurbituril [8] and gold nanorod: targeted phototherapy in combination with SERS imaging on breast cancer cells. *J Phys Chem B*. 2021;125:13415–24.
- Ratkaj I, Mušković M, Malatesti N. Targeting microenvironment of melanoma and head and neck cancers in photodynamic therapy. *Curr Med Chem*. 2022;29:3261–99.
- Shamjith S, Joseph MM, Murali VP, Remya GS, Nair JB, Suresh CH, et al. NADH-depletion triggered energy shutting with cyclometalated iridium (III) complex enabled bimodal Luminescence-SERS sensing and photodynamic therapy. *Biosens Bioelectron*. 2022;204:114087.
- Rahman KMM, Giram P, Foster BA, You Y. Photodynamic therapy for bladder cancers. A focused review. *Photochem Photobiol*. 2023;99:420–36.
- Dhaini B, Wagner L, Moinard M, Daouk J, Arnoux P, Schohn H, et al. Importance of Rose Bengal loaded with nanoparticles for anti-cancer photodynamic therapy. *Pharmaceuticals (Basel)*. 2022;15:1093.
- Sargazi S, ER S, Sacide GS, Rahdar A, Bilal M, Arshad R, et al. Application of titanium dioxide nanoparticles in photothermal and photodynamic therapy of cancer: an updated and comprehensive review. *J Drug Deliv Sci Technol*. 2022;75:103605.
- Taranejoo S, Janmaleki M, Pachenari M, Seyedpour SM, Chandrasekaran R, Cheng W, et al. Dual effect of F-actin targeted carrier combined with anti-mitotic drug on aggressive colorectal cancer cytoskeleton: allying dissimilar cell cytoskeleton disrupting mechanisms. *Int J Pharm*. 2016;513:464–72.
- Chu X, Mao L, Johnson O, Li K, Phan J, Yin O, et al. Exploration of TiO<sub>2</sub> nanoparticle mediated microdynamic therapy on cancer treatment. *Nanomed Nanotechnol Biol Med*. 2019;18:272–81.
- Shrestha A, Hamblin MR, Kishen A. Photoactivated rose bengal functionalized chitosan nanoparticles produce antibacterial/biofilm activity and stabilize dentin-collagen. *Nanomedicine*. 2014;10:491–501.
- Abdulhameed AS, Mohammad AT, Jawad AH. Application of response surface methodology for enhanced synthesis of chitosan tripolyphosphate/TiO<sub>2</sub> nanocomposite and adsorption of reactive orange 16 dye. *J Clean Prod*. 2019;232:43–56.
- Aravind M, Amalanathan M, Mary MSM. Synthesis of TiO<sub>2</sub> nanoparticles by chemical and green synthesis methods and their multifaceted properties. *SN Appl Sci*. 2021;3:409.
- Vichai V, Kirtikara K. Sulforhodamine B colorimetric assay for cytotoxicity screening. *Nat Protoc*. 2006;1:1112–6.
- Pozarowski P, Darzynkiewicz Z. Analysis of cell cycle by flow cytometry. *Methods Mol Biol*. 2004;281:301–11.
- Wlodkowic D, Skommer J, Darzynkiewicz Z. Flow cytometry-based apoptosis detection. *Methods Mol Biol*. 2009;559:19–32.
- Thomé MP, Filippi-Chiela EC, Villodre ES, Migliavaca CB, Onzi GR, Felipe KB, et al. Ratiometric analysis of Acridine Orange staining in the study of acidic organelles and autophagy. *J Cell Sci*. 2016;129:4622–32.
- Justus CR, Leffler N, Ruiz-Echevarria M, Yang LV. In vitro cell migration and invasion assays. *J Vis Exp*. 2014;88:51046.
- Burtis CA, Ashwood ER, Bruns DE. *Tietz Fundamentals of Clinical Chemistry*. 6th ed. St Louis: Elsevier Saunders Company; 2008. (AST, ALT) p. 323–5, (urea, creatinine) p. 363–8.
- Draper HH, Hadley M. Malondialdehyde determination as index of lipid peroxidation. *Methods Enzymol*. 1990;186:421–31.
- Marklund S, Marklund G. Involvement of the superoxide anion radical in the autoxidation of pyrogallol and a convenient assay for superoxide dismutase. *Eur J Biochem*. 1974;47:469–74.
- Habing WH, Pabst MJ, Jakoby WB. Glutathione S-transferases. The first enzymatic step in mercapturic acid formation. *J Biol Chem*. 1974;249:7130–9.
- Khan R, Sultana S. Farnesol attenuates 1,2-dimethylhydrazine induced oxidative stress, inflammation and apoptotic responses in the colon of Wistar rats. *Chem Biol Interact*. 2011;192:193–200.
- Aebi H. Catalase in vitro. *Methods Enzymol*. 1984;105:121–6.
- Sharma R, Ansari MM, Alam M, Fareed M, Ali N, Ahmad A, et al. Sophorin mitigates flutamide-induced hepatotoxicity in wistar rats. *Toxicol*. 2024;243:107722.
- Rice-Evans C, Miller NJ. Total antioxidant status in plasma and body fluids. *Methods Enzymol*. 1994;234:279–93.
- Abu Rakhey MMM, Abd El-Kaream SA, Daoxin Ma. Folic acid conjugated graphene oxide graviola nanoparticle for sono-photodynamic leukemia treatment: up-to-date cancer treatment modality. *J Biosci Appl Res*. 2022;8:28–45.
- Bashir A, Asif M, Saadullah M, Saleem M, Khalid SH, Hussain L, et al. Therapeutic potential of standardized extract of *Mellilotus indicus* (L.) all. And its phytochemicals against skin cancer in animal model: in vitro, in vivo, and in silico studies. *ACS Omega*. 2022;7:25772–25782.
- Adnan M, Akhter MH, Afzal O, Altamimi ASA, Ahmad I, Alossaimi MA, et al. Exploring nanocarriers as treatment modalities for skin cancer. *Molecules*. 2023;28:5905.
- Diaz MJ, Ntarelli N, Aflatooni S, Aleman SJ, Neelam S, Tran JT, et al. Nanoparticle-based treatment approaches for skin cancer: a systematic review. *Curr Oncol*. 2023;30:7112–31.
- Zeng L, Gowda BHJ, Ahmed MG, Abourehab MAS, Chen ZS, Zhang C, et al. Advancements in nanoparticle-based treatment approaches for skin cancer therapy. *Mol Cancer*. 2023;22:10.

37. Kim JA, Åberg C, Salvati A, Dawson KA. Role of cell cycle on the cellular uptake and dilution of nanoparticles in a cell population. *Nat Nanotechnol.* 2012;7:62–8.
38. van Tonder A, Joubert AM, Cromarty AD. Limitations of the 3-(4,5-dimethylthiazol-2-yl)-2,5-diphenyl-2H-tetrazolium bromide (MTT) assay when compared to three commonly used cell enumeration assays. *BMC Res Notes.* 2015;8:47.
39. Noguchi M, Hirata N, Tanaka T, Suizu F, Nakajima H, Chiorini JA. Autophagy as a modulator of cell death machinery. *Cell Death Dis.* 2020;11:517.
40. Wang Y, Kanneganti TD. From pyroptosis, apoptosis and necroptosis to PANoptosis: a mechanistic compendium of programmed cell death pathways. *Comput Struct Biotechnol J.* 2021;19:4641–57.
41. Soldani C, Croce AC, Bottone MG, Frascini A, Biggiogera M, Bottiroli G, et al. Apoptosis in tumour cells photosensitized with Rose Bengal acetate is induced by multiple organelle photodamage. *Histochem Cell Biol.* 2007;128:485–95.
42. Srivastav AK, Mujtaba SF, Dwivedi A, Amar SK, Goyal S, Verma A, et al. Photosensitized rose Bengal-induced phototoxicity on human melanoma cell line under natural sunlight exposure. *J Photochem Photobiol B.* 2016;156:87–99.
43. Karbalaee A, Mohammadalipour Z, Rahmati M, Khataee A, Moosavi MA. GO/TiO<sub>2</sub> hybrid nanoparticles as new photosensitizers in photodynamic therapy of A375 melanoma cancer cells. *J Skin Stem Cell.* 2017;4:63984.
44. Mohammadalipour Z, Rahmati M, Khataee A, Moosavi MA. Differential effects of N-TiO<sub>2</sub> nanoparticle and its photo-activated form on autophagy and necroptosis in human melanoma A375 cells. *J Cell Physiol.* 2020;235:8246–59.
45. Gulla S, Lomada D, Araveti PB, Srivastava A, Murikinati MK, Reddy KR. Titanium dioxide nanotubes conjugated with quercetin function as an effective anticancer agent by inducing apoptosis in melanoma cells. *J Nanostructure Chem.* 2021;11:721.
46. Sharma J, Singh R, Goyal PK. Chemomodulatory potential of flaxseed oil against DMBA/Croton oil-induced skin carcinogenesis in mice. *Integr Cancer Ther.* 2016;15:358–67.
47. Wang Z, Xiao S, Huang J, Liu S, Xue M, Lu F. Chemoprotective effect of boeravinone B against DMBA/Croton oil induced skin cancer via reduction of inflammation. *J Oleo Sci.* 2021;70:955–64.
48. Abdellaoui M, Kadi A, Abrazi Y, Kadi Y, Gary A, Kherfi H, et al. Oral intake of combined natural immunostimulants suppresses the 7,12-DMBA/Croton oil induced two-step skin carcinogenesis in swiss albino mice. *Gulf J Oncolog.* 2023;1:32–41.
49. Das RK, Ghosh S, Sengupta A, Das S, Bhattacharya S. Inhibition of DMBA/croton oil-induced two-stage mouse skin carcinogenesis by diphenylmethyl selenocyanate. *Eur J Cancer Prev.* 2004;13:411–7.
50. Subramanian V, Venkatesan B, Tumala A, Vellaichamy E. Topical application of Gallic acid suppresses the 7,12-DMBA/Croton oil induced two-step skin carcinogenesis by modulating anti-oxidants and MMP-2/MMP-9 in Swiss albino mice. *Food Chem Toxicol.* 2014;66:44–55.
51. Majed F, Nafees S, Rashid S, Ali N, Hasan SK, Ali R, et al. Terminalia chebula attenuates DMBA/Croton oil-induced oxidative stress and inflammation in Swiss albino mouse skin. *Toxicol Int.* 2015;22:21–9.
52. Majed F, Rashid S, Khan AQ, Nafees S, Ali N, Ali R, et al. Tannic acid mitigates the DMBA/croton oil-induced skin cancer progression in mice. *Mol Cell Biochem.* 2015;399:217–28.
53. Divya MK, Salini S, Meera N, Lincy L, Seema M, Raghavamenon AC, et al. Attenuation of DMBA/croton oil induced mouse skin papilloma by Apodytes dimidiata mediated by its antioxidant and antimutagenic potential. *Pharm Biol.* 2016;54:1564–74.
54. Wang J, He Z, Zhao J, Xiao W, Xiong L, Chen W. Anticarcinogenic effect of brucine on DMBA-induced skin cancer via regulation of PI3K/AKT signaling pathway. *Phcog Mag.* 2022;18:29–35.
55. Toomey P, Kodumudi K, Weber A, Kuhn L, Moore E, Sarnaik AA, et al. Intralesional injection of rose bengal induces a systemic tumor-specific immune response in murine models of melanoma and breast cancer. *PLoS ONE.* 2013;8:68561.
56. Chen HJ, Zhou XB, Wang AL, Zheng BY, Yeh CK, Huang JD. Synthesis and biological characterization of novel rose bengal derivatives with improved amphiphilicity for sono-photodynamic therapy. *Eur J Med Chem.* 2018;145:86–95.
57. Jasim AA, Abdulrahman JM, Abd El-kaream SA, Hosny G. Biochemical and pathological evaluation of the effectiveness of nano-targeted sono-photodynamic therapy in breast cancer. *J Biosci Appl Res.* 2019;5:18.
58. Abd El-Kaream SA, Abd Elsamie GH, Abbas AJ. Sono and photo sensitized gallium-porphyrin nanocomposite in tumor-bearing mice: new concept of cancer treatment. *Am J Nanotechnol Nanomed.* 2019;2:5.
59. Abd El-Kaream SA, Abd Elsamie GH, Metwally MA, Almamoori AYK. Sono and photo stimulated chlorine e6 nanocomposite in tumor-bearing mice: upcoming cancer treatment. *Radiol Med Diag Imag.* 2019;2:1.
60. Dhillon SK, Porter SL, Rizk N, Sheng Y, McKaig T, Burnett K, et al. Rose bengal-amphiphilic peptide conjugate for enhanced photodynamic therapy of malignant melanoma. *J Med Chem.* 2020;63:1328–36.
61. Adibzadeh R, Golhin MS, Sari S, Mohammadpour H, Kheirbakhsh R, Mohammadnejad A, et al. Combination therapy with TiO<sub>2</sub> nanoparticles and cisplatin enhances chemotherapy response in murine melanoma models. *Clin Transl Oncol.* 2021;23:738–49.
62. Dardeer AGE, Hussein NG, Abd El-Kaream SA. New garcinia Cambodia as sono/photosensitizer on ehrlich ascites carcinoma bearing mice in presence of dieldrin pesticide as an environmental pollutant. *Int J Innov Sci Res.* 2021;10:1583.
63. Abd El-Kaream SA, Zedan DFM, Mohamed HM, Soliman ASM, El-Kholey SM, Nasra MKE. High-frequency ultrasound-assisted drug delivery of chia, cress, and flax conjugated hematite iron oxide nanoparticle for sono-photodynamic lung cancer treatment in vitro and in vivo. *Cancer Nano.* 2024;15:46.
64. Kim YS, Rubio V, Qi J, Xia R, Shi ZZ, Peterson L, et al. Cancer treatment using an optically inert Rose Bengal derivative combined with pulsed focused ultrasound. *J Control Release.* 2011;156:315–22.
65. Ren W, Yan Y, Zeng L, Shi Z, Gong A, Schaaf P, et al. A near infrared light triggered hydrogenated black TiO<sub>2</sub> for cancer photothermal therapy. *Adv Healthc Mater.* 2015;4:1526–36.
66. Vanerio N, Stijnen M, de Mol BAJM, Kock LM. Biomedical applications of photo- and sono-activated Rose Bengal: a review. *Photobiomodul Photomed Laser Surg.* 2019;37:383–94.
67. Abd El-Kaream SA. Biochemical and biophysical study of chemopreventive and chemotherapeutic anti-tumor potential of some Egyptian plant extracts. *Biochem Biophys Rep.* 2019;18:100637.
68. Abd El-Kaream SA, Abd Elsamie GH, Isewid GA. Laser and ultrasound activated photolon nanocomposite in tumor-bearing mice: new cancer fighting drug-technique. *Arch Oncol Cancer Ther.* 2019;2:1.
69. Abdulrahman JM, Abd Elsamie GH, Al-rawi RAA, Abd El-kaream SA. Antitumor synergistic activity of nano-chlorophyll with sonophotodynamic on Ehrlich ascites carcinoma in mice. *Zanco J Med Sci.* 2020;24:132.
70. Yang CC, Wang CX, Kuan CY, Chi CY, Chen CY, Lin YY, et al. Using C-doped TiO<sub>2</sub> nanoparticles as a novel sonosensitizer for cancer treatment. *Antioxidants (Basel).* 2020;9:880.
71. Dardeer AGE, Hussein NG, Abd El-Kaream SA. New impacts of Garcinia Cambogia as Sono/photosensitizer on Ehrlich ascites carcinoma bearing mice. *Int J Inf Res Rev.* 2021;8:7182.
72. Abd El-Kaream SA, Mohamed HA, El-Kholey SM, Abu Rakhey MMM, ELkallaf AMS, Soliman ASM, et al. Ultrasound allied laser sono-photobiomodulation activated nano-curcumin: up-and-coming selective cancer cell killing modality. *BioNanoSci.* 2023;13:49–65.
73. Abd El-Kaream SA, Mohamad AA, El-Kholey SM, Ebied SAE. Electroporation assisted delivery of Roussin salt porphyrin-based conjugated carbon nanoparticles for sono-X-ray-photodynamic prostate cancer in vitro and in vivo treatment. *Cancer Nano.* 2025;16:3.
74. Arora N, Koul A, Bansal MP. Chemopreventive activity of Azadirachta indica on two-stage skin carcinogenesis in murine model. *Phytother Res.* 2011;25:408–16.
75. Padhy I, Paul P, Sharma T, Banerjee S, Mondal A. Molecular mechanisms of action of eugenol in cancer: recent trends and advancement. *Life (Basel, Switzerland).* 2022;12:1795.
76. Abd El-Kaream SA, Hussein NGA, El-Kholey SM, Elhelbawy AMAEI. Microneedle combined with iontophoresis and electroporation for assisted transdermal delivery of *goniothalamus macrophyllus* for enhancement sonophotodynamic activated cancer therapy. *Sci Rep.* 2024;14:7962.

## Publisher's Note

Springer Nature remains neutral with regard to jurisdictional claims in published maps and institutional affiliations.